

**Investigation of Thin Liquid Films during Low Salinity
Waterflooding in Carbonates by using Molecular
Dynamics Simulation**

By

Askhat Abdrakhmanov

2020

Thesis submitted to the School of Mining and Geosciences of Nazarbayev
University in Partial Fulfillment of the Requirements for the Degree of
Master of Science in Petroleum Engineering

Nazarbayev University
April 2020

Acknowledgments

I wish to express my deepest gratitude to my supervisors, Dr. Ali Shafiei, for his guidance and support during my time pursuing the master's degree. I also would like to thank my co-supervisor Dr. Jalal Foroozesh, Universiti Teknologi PETRONAS in Malaysia, for his valuable comments and advice during the course of conducting this research work. Special thanks to Dr. Yanwei Wang for useful meetings and for sharing his knowledge on the basic theory and methods of molecular dynamics simulations.

I would like to thank Dr. Peyman Pourafshary and Dr. Muhammad Hashmet reviewing my thesis and for their constructive comments which improved the quality of writing of this report. I also would like to express my appreciation to the rest of the academic staff of the petroleum engineering department including Prof. Randy Hazlett, Dr. Lei Wang, and Dr. Sonny Irawan.

This work was part of the Faculty Development Competitive Research Grants Program (FDCRGP) grant entitled: "LSWF: Experimental and Modeling Investigation of Low Salinity Water Flooding in some Oil fields of Republic of Kazakhstan – Improved Oil Recovery Implications." I wish to acknowledge the financial support I received from this grant.

I would like to acknowledge the National Supercomputing Center in Shenzhen, China, for providing the computational resources and Materials Studio (version 7.0, module Forcite).

I want to thank my research teammates, Medet Yerkin and Zhambyl Sarbas, with whom I worked daily and shared all ups and downs along the way.

And last but not least, I want to thank my parents, Alkhadi Suttibayev and Zhanar Zhagiparova, who are the two people in my life that I want to make the most proud of me.

Originality Statement

I, Askhat Abdrakhmanov, hereby declare that this submission is my own work and to the best of my knowledge it contains no materials previously published or written by another person, or substantial proportions of material which have been accepted for the award of any other degree or diploma at Nazarbayev University or any other educational institution, except where due acknowledgment is made in the thesis.

Any contribution made to the research by others, with whom I have worked at NU or elsewhere is explicitly acknowledged in the thesis.

I also declare that the intellectual content of this thesis is the product of my own work, except to the extent that assistance from others in the project's design and conception or in style, presentation, and linguistic expression is acknowledged.

Signed on 15.04.2020

Abstract

In the past two decades or so, Low Salinity Waterflooding (LSWF) has been the subject of interest and a hot research topic among EOR scientists as a promising EOR method considering its low capital and operating costs combined with its minimal environmental footprint. Despite all of the theories, laboratory observations, and explanations mentioned above on mechanism of wettability alteration in carbonate rocks surface, chemiophysical interaction between ions and rock surface during LSWF is still ambiguous. A universally applicable mechanism for low salinity effect in carbonates is not accepted, yet. The effect of each component on wettability alteration is still being debated. This can be attributed to the fact that most experimental studies use different rocks, crude oils, and test procedures. Besides, complex interactions between minerals, crude oil and brine may cause confusion about uncovering the major mechanism behind wettability alteration during LSWF in each case. Hence, new theoretical scientific investigations at various scales including the molecular scale are needed to shed light on unknown aspects of some major mechanisms proposed for LSWF in carbonate reservoirs. In addition, a basic scientific understanding of the unknown causes of low salinity effect in carbonates will contribute to the development of better experimental investigations and reservoir modeling and simulation works which can pave the road for design and implementation of field trials and eventually full field implementation of the process in carbonates. In this study, we used Molecular Dynamics Simulation (MDS) approach to shed light on the interaction of molecules during LSWF on calcite rock at (1014) cleavage plane. We investigated the effect of brine salinity on brine film thickness and stability on a calcite surface by using MDS. Also, the behavior of individual ions (Na^+ , Cl^- , SO_4^{2-} , Mg^{2+} , and Ca^{2+}) during LSW was investigated. The presence of polar components and their effect on brine film stability were also investigated. For this purpose, simulations were performed for high salinity brine, low salinity brine, and deionized water at molecular scale. The results showed that as the salinity of brine decreases, water film on the calcite surface expands rendering the surface more water-wet. Change in the thickness of water film was attributed to the formation of electric double layers. Electrostatic interaction between positively charged Stern layer and negatively charged diffuse layer affects the brine thickness. The results also showed stronger adhesion of polar components in oil to the oil/brine interface in the high salinity brine compared to low salinity brines, which agrees with the ion bridging mechanism during multicomponent ion-exchange.

Table of Contents

TABLE OF CONTENTS	V
LIST OF FIGURES	VII
LIST OF TABLES	VIII
1. INTRODUCTION	9
1.1 Background	9
1.2 Problem definition.....	11
1.3 Objectives of the thesis	11
1.4 Research methodology	12
1.5 Thesis structure	12
2. LITERATURE REVIEW	13
2.1 Conventional waterflooding.....	13
2.2 Laboratory studies on LSW in carbonates	13
2.2.1 Effect of ions.....	15
2.2.2 Effect of polar components in crude oil.....	17
2.3 Field tests of LSW on carbonate reservoirs.....	18
2.4 Wettability alteration mechanisms	19
2.4.1 Multicomponent ion exchange (MIE)	19
2.4.2 Rock dissolution.....	20
2.4.3 Double layer expansion.....	22
2.4.4 Change of pH.....	22
2.5 Modeling of LSWF	23
2.6 Molecular dynamics simulations of low salinity waterflooding	24
3. MOLECULAR DYNAMICS SIMULATION	29
3.1 Basics of molecular dynamics simulation	29
3.1.1 Bonding interaction	29
3.1.2 Van der Waals interaction.....	30
3.1.3 Electrostatic interaction	30
3.1.4 Periodic boundary.....	31
3.1.5 Simulation time step	32
3.1.6 Radial distribution functions	33
3.1.7 Interaction energy	34
3.2 Simulation parameters.....	35
4. RESULTS AND DISCUSSION	40

5.1	Initial equilibration.....	40
5.2	Radial distribution function.....	41
5.3	Brine thickness	42
5.4	Distribution of ions in the brine	44
5.5	Distribution of polar components in oil	46
5.6	Interaction energy.....	47
5.	CONCLUSIONS AND RECOMMENDATIONS	48
	NOMENCLATURE	49
6.	REFERENCES	52
	APPENDIX A	57

List of Figures

Figure 1. Oil recovery curve for different dilutions of seawater (Yousef et al, 2011).....	14
Figure 2. Wettability alteration mechanism (Emad and Sepehrnoori, 2016).....	20
Figure 3. Illustration of simulation structure developed by Zhao et al (2018)	26
Figure 4. Distribution of molecules after equilibration, charged inner surface (Zhao et al, 2018).....	26
Figure 5. Distribution of molecules after equilibration neutral inner surfaces (Zhao et al, 2018).....	27
Figure 6. Behavior of water droplet on the calcite surface. (Chang et al, 2018)	27
Figure 7. Schematic representation of periodic cells for a cubic system in two dimensions (Leach, 2001).....	32
Figure 8. Graphical representation of collision simulation between two atoms by using different time steps. Small time step (left), large time step (center), appropriate time step (right). (Leach, 2001).....	33
Figure 9. Radial distribution function derived from the MDS of liquid argon (Barrat and Hansen, 2003).....	34
Figure 10. 3D illustration of calcite crystal. (green: calcite, red: oxygen, grey: carbon).....	35
Figure 11. Side view of calcite crystal	36
Figure 12. Illustration of molecules used in simulation: water, decane and heptanoic acid. (from top to bottom) (white: hydrogen, red: oxygen, grey: carbon)	37
Figure 13. Initial configuration of the simulation cell with deionized water.....	38
Figure 14. Snapshots of the simulation cells after energy minimization (pale green: chlorine, violet: sodium, yellow: sulfur, olive: magnesium).....	40
Figure 15. The total energy of the DIW case at different energy optimization step.....	41
Figure 16. Radial distribution function between calcite and water molecules	42
Figure 17. Relative concentration profile of water molecules.....	43
Figure 18. Relative concentration profile of oil molecules.....	44
Figure 19. Concentration profile of ions in HS brine	45
Figure 20. Concentration profile of ions in HS brine	45
Figure 21. Concentration profile of heptanoic acid molecules for HS case	47

List of Tables

Table 1. Number of ions dissolved in the aqueous phase for three cases studied.....	37
Table 2. Results for calculation of the difference in interaction energy.	47
Table 3. Calculation for the difference in interaction energy	57

1. Introduction

In this chapter after providing a short background and explaining the importance and relevance of the project to the petroleum industry the thesis problem statement and objectives of the research are presented. Then the methodology used for conducting this research is briefly discussed followed by introduction of different chapters and structure of this thesis.

1.1 Background

More than half of the world's proven oil reserves are found in carbonate reservoirs. However, oil recovery from these reservoirs rarely exceeds 40%. This is partly because carbonate reservoirs naturally have oil-to-mixed wettability, contains natural fractures, have low matrix permeability, and are highly heterogeneous because of their geology (Cueic, 1984). Low Salinity Waterflooding or LSWF is an EOR method which can be used to increase the recovery of oil. LSWF is popular due to the low capital and operating costs combined with its minimal environmental footprint (Morrow and Buckley, 2011). This method is also known by other names, such as Designer Waterflood by Shell, Smart waterflooding by Saudi Aramco, LoSal™ by British Petroleum (BP), or Advanced Ion Management by Exxon Mobil (Bartels et al, 2019).

Conventional waterflooding is mainly used for reservoir pressure maintenance and generally applied after the primary recovery period is over. The composition of connate water is usually different from the composition of the injected brine. Multiple laboratory studies have shown that adjusting the composition of injected brine oil recovery from the core can be improved (Webb, Black and Tjetland, 2005; Rivet, 2009; Fjelde, Asen and Omekeh, 2012). Changing the brine composition alters the thermodynamics equilibrium between rock and brine, which leads to wettability alteration of the rock. (Tang and Morrow, 1999)

Several researchers reported on the effectiveness of LSWF in both carbonate and sandstone rocks from both laboratory and field studies (Webb, Black and Tjetland, 2005; Rivet, 2009; Fjelde, Asen and Omekeh, 2012). LSWF can lead to additional oil recovery up to 25% in carbonate rocks. Multiple researchers have concluded that low salinity brine changes shape and endpoints of the relative permeability curve resulting in higher relative permeability of oil and lower relative permeability of water (Fjelde, Asen and Omekeh, 2012). BP conducted an LSWF project in the Endicott sandstone oil field in Alaska and increased oil recovery by 26% (Seccombe et al, 2010). BP, Shell, Chevron, and ConocoPhillips are running LSWF projects in

the Clair Ridge oil field in the North Sea. The project is expected to produce an additional 40 million barrels of oil at relatively low capital investment. However, LSWF is not widely popular because the mechanism behind additional oil recovery is still unclear. The results from experiments conducted by several oil companies like BP, Shell, Saudi Aramco and PetroChina showed that in some cases LSWF may increase additional oil recovery by 5-25% (Yousef et al, 2011; Xie et al, 2014; Seccombe et al, 2010), but in other cases additional oil recovery was negligible (Suijkerbuijk et al, 2014).

The consensus is that wettability alteration in the system towards water-wet condition leads to additional oil recovery, but phenomenon causing wettability alteration is partly unknown (McGuire et al, 2005; Later et al, 2007; Nasralla, Bataweel and Nasr-el-Din, 2011; Skrettingland et al, 2011; Emadi and Sohrabi, 2013). Electrical double layer expansion (DLE) and multi-component ion exchange (MIE) are two widely accepted mechanisms responsible for the change in wettability in the system. (Lager et al, 2008; Lee et al, 2010; Nasralla and Nasr-El-Din, 2011) However, other mechanisms were also suggested by other authors, such as fine mobilization (Tang and Morrow, 1999), rock dissolution (Lager et al, 2008) and migration of natural surfactants in the oil (Sohrabi et al, 2017). According to Austad et al (2018), presence of SO_4^{2-} in brine is important for wettability alteration, because SO_4^{2-} acts as a catalyst for wettability alteration. Several studies have shown that lowering the salinity of injected brine does not necessarily lead to a reduction in interfacial tension (IFT) between aqueous and oleic phase, rather there exists a critical salinity at which IFT between the two phases is minimum (Vijapurapu and Rao, 2004; Alotaibi and Nasr-el-Din, 2009). Some other researchers have also indicated that the double-layer expansion, caused by the change of zeta potential at brine/oil and oil/rock interfaces, leads to wettability alteration (Mahani et al, 2015).

Buckley and Liu suggested that electrostatic interactions can bind and/or bridge ions at both oil/rock and oil/brine interfaces. Another study showed that change in the composition of brine leads to alterations in the wettability of the rock (Chiappa et al, 1999). The presence of divalent ions increased the adsorption of organic components in the oil onto the rock surface allegedly through the ion-bridging mechanism. A study conducted by Zhang, Xie and Morrow (2007) reported that wettability alteration towards a water-wet state occurs if imbibing brine contains SO_4^{2-} and Ca^{2+} or Mg^{2+} . Their results showed that the effect of Mg^{2+} as water alternating agent significantly enhanced as the temperature increased. Another experiment conducted by Awolayo, Sarma and Alsumaiti (2014), also concluded that increase in SO_4^{2-} concentration in injected brine contributes to oil recovery up to a certain limit in coreflooding

tests performed on carbonate rocks from the Middle East. They have reported that increasing SO_4^{2-} concentration in injected brine beyond four times adversely affects the LSWF performance. However, we argued that the sulfate ions increase the electrostatic repulsive forces between two interfaces which generates an expansion of the electrical double layer.

1.2 Problem definition

Despite all of the theories, laboratory observations, and explanations mentioned above on mechanism of wettability alteration in carbonate rocks surface, chemiophysical interaction between ions and rock surface during LSW is still ambiguous. A universally applicable mechanism for low salinity effect in carbonates is not accepted, yet. The effect of each component on wettability alteration is still being debated. This can be attributed to the fact that most experimental studies use different rocks, crude oils, and test procedures. Besides, complex interactions between minerals, crude oil and brine may cause confusion about uncovering the major mechanism behind wettability alteration during LSW in each case. The puzzle of the mechanism behind wettability alteration during LSW prevents the widespread field application of this cheap and simple IOR/EOR method. This is mainly due to the uncertainties imposed on selecting the optimum brine for the candidate reservoir and not being able to predict the target reservoir's reaction to the LSW and more importantly not being able to predict the incremental recovery factor which impacts the economic viability of the project. Therefore, new studies at various scales including the molecular scale are needed to shed light on unknown aspects of some major mechanisms proposed for LSW in carbonate reservoirs. Moreover, a basic scientific understanding of the unknown causes of low salinity effect will contribute to the development of better experimental investigations and reservoir modeling and simulation works which can pave the road for design and implementation of field trials and eventually full field implementation of the process. In addition, it can help to screen and identify the most suitable candidates for this EOR method.

1.3 Objectives of the thesis

The main objective of this thesis project was to investigate the effect of brine salinity on brine film thickness and stability on a calcite surface by using the molecular dynamics simulation. Also, the behavior of individual ions (Na^+ , Cl^- , SO_4^{2-} , Mg^{2+} , and Ca^{2+}) during LSW was studied. The presence of polar components and their effect on brine film stability was investigated. To achieve the objectives of the project effect of brine salinity and composition on wettability

alteration during LSWF was also analyzed. The brine thickness was measured at different salinities on a calcite surface. The arrangement of polar oil components at different salinities was studied, as well.

1.4 Research methodology

The Material Studio software was used to construct and run the molecular dynamics simulations. Molecular dynamics simulations enable us to investigate systems and predict their macroscopic properties by considering microscopic replication of the system with a manageable amount of atoms or molecules. Radial distribution function was used to describe the relationship between the brine film and calcite surface. Also, interaction energies between the liquid phases and rock surface were calculated.

1.5 Thesis structure

This thesis is organized in five chapters, namely, the introduction, literature review, methodology, results and discussion, and conclusions and recommendations. In the literature review chapter, the current state of knowledge on low salinity water flooring in the literature is briefly presented and critically discussed. The methodology chapter describes the process of molecular dynamics simulation development and its analysis. In the next two chapters the results obtained are presented and interpreted to explain the wettability alteration. In the final chapter conclusions and recommendations attained from the research are provided.

2. Literature review

2.1 Conventional waterflooding

Conventional waterflooding is the most commonly used secondary oil recovery technique which improves recovery by injecting water into the reservoir. Injected water maintains the initial reservoir pressure and improves the oil recovery by sweeping the crude oil towards the production wells. In some cases waterflooding can be used to mitigate surface subsidence, as can be seen from cases of Wilmington (US) and Ekofisk (North Sea) oilfields (Raymond and Leffler, 2006). The main advantage of the method is that water is inexpensive and water is readily available in most oil fields (rivers, oceans, or aquifer wells). The success of a waterflooding project depends on multiple factors, including reservoir depth, porosity, lithology, reservoir geometry, permeability, heterogeneity of the reservoir rock properties, fluid properties, operating cost, availability of the injected water, and environmental footprint. (Raymond and Leffler, 2006). Conventional waterflooding can increase oil recovery by up to 60% of the initial oil in place (Baviere, 1991). Conventional waterflooding is the most effective in water-wet reservoirs since water can in such conditions enter the small pores and sweep the residual oil from them. In oil-wet reservoirs, water cannot enter small pores and travels through the larger pores, which in turn leads to early water breakthrough. For carbonate reservoirs, which are generally are oil-wet and highly fractured, water flow flows through the high permeable fractures and does not sweep oil from the rock matrix.

2.2 Laboratory studies on LSW in carbonates

In the beginning composition of the injected brine was not considered as the main parameter affecting the oil recovery. First improved oil recovery due to LSW was observed by Tang and Morrow (1999). Since then many studies were conducted to identify, reproduce and explain the mechanism behind improved oil recovery. Initially, it was believed that a low salinity effect can be observed only in sandstones. Until LSW was successfully implemented in the coreflooding of carbonate cores by Yousef, Al-Saleh and Al-Jawfi (2012). Austad (2013) has found that optimizing the ionic composition of the injected brine leads to improved oil recovery in carbonate cores. Change in wettability contributed to the oil displacement from the porous matrix of the rock (Austad, 2013).

In the study performed by Yousef et al (2011) diluted seawater was used to increase oil recovery by coreflooding. Stepwise dilution of injected seawater in tertiary mode leads to an increase in oil recovery by 17.6% OOIP compared to undiluted seawater injection at secondary mode. The detailed results can be seen in Figure 1. The study showed that wettability can be altered without SO_4^{2-} , Ca^{2+} , and Mg^{2+} contribution. The study demonstrated the importance of tuning monovalent ions in the brine to achieve a low salinity effect.

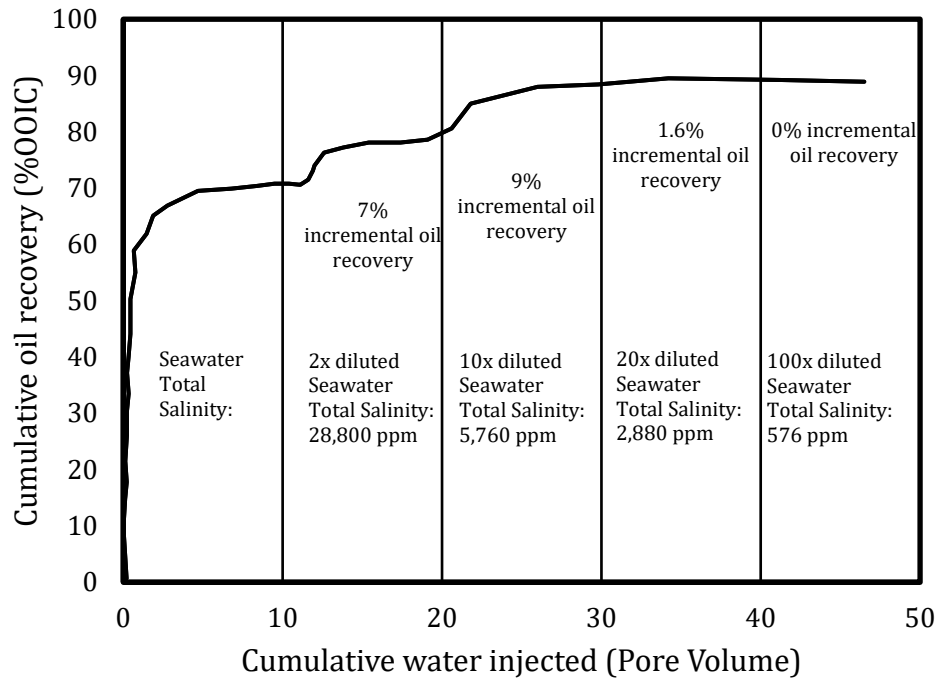


Figure 1. Oil recovery curve for different dilutions of seawater (Yousef et al, 2011)

In another study done by Zahid, Shapiro and Skauge (2012), Aalborg chalk core plugs and reservoir carbonate core plugs were flooded by different dilution of seawater. LSW was not effective in reservoir core plugs at room temperature. However, when the temperature was increased to 90°C, LSW led to a significant increase in oil recovery. This is believed to be due to the higher activity of key ions at high temperatures. Meanwhile, LSW of chalk core plugs did not lead to improved oil recovery both at room and reservoir temperature. NMR results showed no significant change in the T2 distribution peak for any of the cores, which indicates that surface relaxation was not achieved with low salinity brines. The pressure drop across reservoir core plugs increased significantly with a decrease in salinity of injected brine, which authors attributed to fine migration. However, low salinity injection at room temperature did not lead to improved oil recovery which suggests that fines migration does not always result in improved microscopic efficiency. Additionally, the effluent of coreflooding of reservoir core

plug with low salinity brine at 90°C indicated constant concentration of Ca^{2+} , which was absent at low salinity brine injection at room temperature. This suggests that dissolution also contributed to improved oil recovery. Though authors admitted that results could be deviated due to the influence of capillary end effect as pressure drop increases during LSW in carbonate plug cores.

2.2.1 Effect of ions

Spontaneous imbibition experiments showed that sulfate ions play a major role in the wettability alteration of carbonates from mixed-wet to water-wet (Hognesen, Strand and Austad, 2005). Experiments were conducted on outcrop chalk cores, limestone cores, formation water, and seawater. Their work showed that high SO_4^{2-} concentration in injected brine leads to improved oil recovery at high temperatures (Hognesen, Strand and Austad, 2005). In another study conducted by Webb, Black and Tjetland (2005), chalk cores from the Valhall oil field in the North Sea were injected by seawater rich in sulfate ions which lead to a change of wettability to the more water-wet condition compared to formation water which has a low concentration of sulfate ions. Spontaneous imbibition by seawater resulted in 40% more oil recovery compared to spontaneous imbibition by formation water. Capillary pressure curves showed that at any given pressure oil saturation was lower for imbibition with seawater than for imbibition with formation water. Also, forced injection of sulfate-rich seawater resulted in lower residual oil saturation compared to forced injection of sulfate-free formation water (Webb, Black and Tjetland, 2005).

A study conducted by Zhang, Xie and Morrow (2007) revealed that wettability alteration towards a water-wet state occurs if imbibing brine contains SO_4^{2-} and Ca^{2+} or Mg^{2+} . In this study, imbibition tests were performed on chalk cores using oil with the acid number (AN) of 2.08 mgKOH/g and modified brines from the Ekofisk oil field in the North Sea with different SO_4^{2-} , Ca^{2+} , and Mg^{2+} concentrations. The tests were performed at 70, 100, and 130 °C. The results showed that the effect of Mg^{2+} as water alternating agent significantly enhanced as temperature increased.

Strand et al (2008) studied wettability alteration of chalk cores using a crude oil with AN of 1.9 mgKOH/g. Their work verified the alteration of wettability towards more water-wet state when seawater is used as imbibing liquid, which resulted in improved oil recovery by 14% OOIP compared to the imbibition of formation water with low sulfate ion concentration. In another study by Strand, Puntervold and Austad (2008), limestone cores were used as porous

media. In this study, spontaneous imbibition by seawater resulted in higher oil recovery (an increase of 15% OOIP) compared to brine free of SO_4^{2-} . Also, wettability measurements based on chromatographic separation of components showed that adsorption of SO_4^{2-} has a similar effect on both limestone and chalk cores.

Gupta et al (2011) performed coreflooding experiments on limestone and dolomite cores. In their experiments, authors added borate, sulfate, and phosphate ions to injected brine in the tertiary mode after secondary mode flooding with formation water. Also, softened water was used as the injected fluid in tertiary mode. The coreflooding of non-fractured limestone and dolomite cores with seawater containing added sulfate ions increased recovery by 5-9% OOIP compared to waterflood with formation water. The coreflooding of limestone core with softened formation water resulted in incremental 7-9% OOIP recoveries compared to waterflood recoveries using unmodified formation water. Using seawater with added phosphate ions and removed sulfate ions as injected fluid in limestone cores resulted in incremental oil recovery of 20% OOIP compared to formation water flooding, whereas using seawater with added borate ions lead to increase in oil recovery by 15% OOIP. Gupta et al (2011) concluded that softening (removing of Ca^{2+} and Mg^{2+} ions) of injected fluid contributes to dissolution which is one of the proposed mechanisms for wettability alteration in carbonate rocks.

Chandrasekhar and Mohanty (2013) showed that Ca^{2+} does not contribute to wettability alteration in carbonates during LSW. In their experiments on limestone reservoir rocks at 248 °F, injection of seawater with added Mg^{2+} and SO_4^{2-} and diluted seawater contributed to wettability alteration and hence improved oil recovery. However, the addition of only Ca^{2+} did not lead to an improvement in oil recovery, hence it did not contribute to wettability alteration. The authors concluded that the desorption of organic acid groups due to mineral dissolution and multi-ion exchange was responsible for wettability alteration.

Al-Attar et al (2013) performed coreflooding tests on carbonate core plugs from the Bu Hasa oil field in Abu Dhabi. The results of their experiments showed that using diluted seawater as injected fluid can improve oil recovery. Salinity reduction from 197,362 ppm to 5000 ppm led to an increase in oil recovery from 63% to 84.5% OOIP. From contact angle measurements, they have concluded that wettability alteration from oil-wet to intermediate-wet was the reason for improved oil recovery. Additionally, the authors concluded that the addition of Ca^{2+} to injected brine adversely affects the oil recovery process. Also, the authors found a limit for sulfate ion concentration (47 ppm in 5000 ppm formation water) after which sulfate ion addition

negatively affects the oil recovery process. The authors reported that the interfacial tension of the oil-brine system does not contribute to LSW performance. Another work performed by Awolayo, Sarma and Alsumaiti (2014) also concluded that increase in SO_4^{2-} concentration in injected brine contributes to oil recovery up to a certain limit in coreflooding tests performed on carbonate rocks from the Middle East. They have found that increasing SO_4^{2-} concentration in injected brine beyond four times adversely affects the LSW performance. Authors argued that sulfate ions increase electrostatic repulsive forces between two interfaces which generates an expansion of the electrical double layer.

2.2.2 Effect of polar components in crude oil

Mwangi et al (2018) tested the effect of surface acting compounds (SAC) dissolved in oil on the wettability of the carbonate rock surface. In their work, they modeled oil by dissolving different organic acids in pure decane and measured wettability alteration by a modified flotation technique (MFT). In the MFT, rock grains are aged in water for several days. Then, oil is added and the mixture of oil-water-rock is stirred. Finally, the mixture is allowed to settle so that oil-wet rock covered with oil will be suspended in the oil phase, while water-wet rock will settle down at the bottom of the water phase. If the rock is fractional-wet, then part of the rock will be suspended in the oil phase while other parts will sink in the water phase. In the end, rock quantities suspended/sunk are weighed to measure the percentage of rocks suspended in the oil phase. In their study, they conducted experiments on chalk, dolomite and limestone rocks. Three SACs were used, namely, acetic acid, myristic acid, and heptanoic acid. MFT results for decane, rock, and deionized water system showed that 69% for limestone, 75% for dolomite, and 88% of chalk grains were in the oil phase at 70°C. At 110 °C fractional oil wettability increased to 75%, 79%, and 92% respectively. Initial oil wetness of the system can be explained by weak dipole moment which exists between carbon and hydrogen atoms, which generates weak polar charge in decane molecule. This polar charge in the absence of strongly charged ions in brine causes decane to adhere to the charged rock surface. As the salinity of brine was increased, wettability shifted towards the water-wet condition. Namely at 70 °C and salinity of 10,000 ppm fractional oil wettability was 15% for chalk, 13% for dolomite and 23% for limestone. The shift towards water-wet condition is explained by the stronger interaction between ions in water and rock surface compared to interaction between weakly charged decane molecule and rock surface.

The effect of acetic acid on the rock's wettability is negligible at room temperatures, but at higher temperatures shift in wettability of the rock is much larger. At high salinities

(100,000 and 10,000 ppm) wettability of the rock shifts to oil-wet. Meanwhile, at low salinities (1000 and 0 ppm) wettability changes to water-wet. However, myristic acid and heptanoic acid showed the opposite trend compared to acetic acid. The addition of these acids at high salinities resulted in more water-wet condition and shifted to the oil-wet condition as salinity decreased. Authors assume that polar organic acids in oil adhere to charged carbonate surface and contribute to the oil-wetness of the rock. At high salinities, inorganic ions in brine would compete for surface sites weakening organic acid bonding with the surface and shifting it to water-wet condition. In their work authors showed that presence long-chain acids in the oil, like myristic and heptanoic acid, contribute to oil-wetness of the rock, but the dilution of short-chain acids in oil yielded more water-wet rock surface. Authors supposed that acetic acid had the opposite effect on wettability compared to other acids because it is more soluble in water than in decane and transported from the oil phase to the aqueous phase. Through their work authors showed that the composition of oil greatly influences wettability alteration during low salinity waterflooding.

2.3 Field tests of LSW on carbonate reservoirs

The first field-scale test of LSW on carbonate rock was performed by Yousef, Al-Saleh and Al-Jawfi (2012). The authors have performed two single-well chemical tracer tests on two wells in a carbonate reservoir using diluted seawater. In their work, the authors tested a carbonate reservoir by injecting diluted seawater and measured residual saturations by a single-well chemical tracer test. Stepwise increasing dilutions of seawater were injected in tertiary mode. The first well was injected in three steps over four weeks period. Firstly, large amounts of seawater were injected to remove any movable oil in the vicinity of the well. The second step was used to confirm that residual oil saturation was achieved. In the third step, ten times diluted seawater was injected to demonstrate the effectiveness of LSW. Injection of diluted seawater leads to a decrease in residual oil saturation by 7 saturation units. The second well was also tested in three stages over four weeks period. In the first stage, seawater was injected to achieve residual oil saturation. In the second stage twice diluted seawater was injected. By injection of twice diluted seawater reduction of 3 saturation units was achieved. In the third stage, ten times diluted seawater was injected to reduce residual oil saturation by another 3 saturation units. Overall, a reduction of 6 saturation units was achieved in the second well, which is comparable with the results of the first well.

2.4 Wettability alteration mechanisms

Most researchers believe that wettability alteration in carbonate rocks happens due to the dissolution of rock matrix or change in surface charge of the rock. Regarding changing the surface charge of the rock, adsorption of sulfate ions was proposed by some authors as the primary mechanism for wettability change. Strand et al (2008) performed spontaneous imbibition tests on different carbonate rocks with brine containing various concentrations of sulfate ions in the presence/absence of cationic surfactant. The results have shown that at high temperatures and up to a certain limit in concentration, sulfate ions are effective in changing wettability in the presence of cationic surfactants. The authors proposed that the adhesion of sulfate ions to the surface of rock creates a negative layer, which contributes to the removal of adsorbed carboxylic material from rock by surfactants. Also, their work showed that spontaneous imbibition by sulfate-rich brine is more pronounced in chalk core compared to the dolomite core. Contact angle measurements showed the same effect.

Similar research was conducted by Hognesen, Strand and Austad (2005), where they studied the effect of sulfate concentration in seawater on the performance of cationic surfactant. This study also showed that the presence of surfactants in sulfate-rich brine contributes to oil recovery at high temperatures (90 – 130°C). Although in the previous study, Strand et al (2008) concluded that sulfate ion concentration was limited to 1g/L, in this study sulfate concentration of 2.31 g/L was still effective as a catalyst. The authors suggested that sulfate acts as a catalyst because of a higher affinity to the surface of carbonates at high temperatures. They, also, stated that sulfate adsorption will change the surface charge of the rock and expels carboxylic groups from the rock. According to the authors, in addition to wettability alteration, surfactants and sulfates contribute to IFT lowering, which also increases oil recovery. Also, the authors stated that it is crucial to know Ca^{2+} concentration in the connate brine to prevent CaSO_4 precipitation.

2.4.1 *Multicomponent ion exchange (MIE)*

In a research done by Zhang, Tweheyo and Austad (2006), a low salinity effect on carbonate rocks was reached by using brine containing sulfate ions and calcium or magnesium ions at temperatures higher than 90°C. They proposed two mechanisms for change in wettability for carbonate rocks represented in Figure 2. In the first case, at low temperatures, Mg^{2+} is less active than Ca^{2+} , which may cause CaSO_4 precipitation and weak wettability alteration. In the second case, as temperature increases sulfate ions tend to adhere to the surface of chalk rocks. At the same time, Ca^{2+} adsorption to the surface increases and positive charge of the surface

weakens. Therefore, Ca^{2+} ions are concentrated near the surface of the rock, where they react with carboxylic material of the oil and contribute to their release from the surface. As temperature increases, Mg^{2+} becomes more active than Ca^{2+} and SO_4^{2-} . Hence, Mg^{2+} substitutes with Ca^{2+} causing the release of carboxylic material from the surface. However, at low temperatures, Ca^{2+} reacts with sulfate and precipitation reaction occurs, which adversely affects the injection of the fluid.

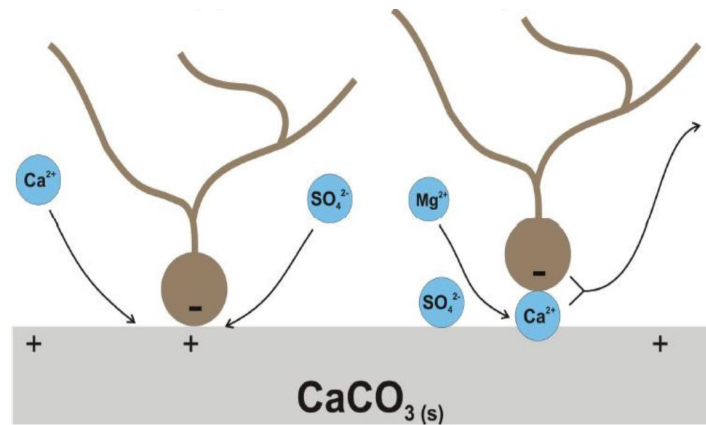


Figure 2. Wettability alteration mechanism (Emad and Sepehrmoori, 2016)

Previous authors suggested that wettability alteration is caused by the presence of calcium, magnesium and sulfate ions. Moreover, the authors suggested chemical mechanisms of ions interaction with the surface and following release of carboxylic material from the surface, rendering the surface water-wet. According to this mechanism, at high temperatures sulfate acts as a catalyst and creates an excess of calcium ions in the vicinity of the surface. Lager, Webb and Black (2007), also, proposed a multi-component ion exchange mechanism where a carboxylic group is detached by ions in the brine. According to this proposed mechanism, wettability is solely dependent on the ionic composition of the brine and is not affected by the salinity of the brine.

2.4.2 Rock dissolution

During the mineral dissolution process, pore space collapses. Consequently, oil is expelled from the rock. In the coreflooding experiments performed by Tang and Kovscek (2004) improved oil recovery was correlated with the production of fines at high temperatures. In another study by Schembre and Kovscek (2004), it was suggested that during the LSW oil-wet surface of the rock dissolves and reveals the water-wet surface behind it. In the work done by Schembre, Tang and Kovscek (2006), the dissolution mechanism was proposed for wettability alteration.

Strand et al (2008) observed that during seawater flooding of limestone core at high temperatures concentration of Ca^{2+} increased in effluent fluid, whereas the concentration of Mg^{2+} decreased. Also, they noticed that the mechanical strength of the core weakened. These led to the conclusion that Mg^{2+} ions substituted Ca^{2+} ions in the lattice of the rock. Since Mg^{2+} ions are larger than Ca^{2+} this created stress in the lattice and weakened core structure. Moreover, Austad et al (2008) suggested that higher solubility of MgCO_3 in the water at high temperatures compared to CaCO_3 further deteriorates the mechanical integrity of the rock. In another work, Mahani et al (2015) studied the effect of LSW on dolomite and limestone cores by conducting zeta potential and contact angle measurements. In their work, they showed that LSW is effective without any dissolution. Also, contact angle and zeta potential measurements showed that limestone has a stronger response to low salinity brine injection compared to dolomite.

In another work done by Yousef, Al-Saleh and Al-Jawfi (2012), researchers investigated a low salinity effect on carbonate cores using NMR, zeta potential and contact angle measurements. Zeta potential measurements showed that as the salinity of the brine decreased, zeta potential shifted to the negative-state, which shows that surface charge of the carbonate was significantly altered. NMR tests of all core samples showed that shorter T_2 times after injecting brine with different salinities, which indicates fast surface relaxation. An increase in relaxivity of surface contributes to the relaxation of excited protons on the pore surface, therefore decreasing salinity of injected brine can alter surface charge of the rock. NMR results also showed improved connectivity between micropores and macropores. Also, flooding with deionized water and measuring the concentration of ions in the effluent indicated constant concentration of Ca^{2+} and SO_4^{2-} even after 35 pore volumes of deionized water were injected. These authors suggested that anhydrite dissolution resulted in better connectivity of pores and the production of ions in the effluent of deionized water injection. Also, anhydrite dissolution is the source of in-situ SO_4^{2-} generation, which may further enhance wettability alteration in the system. Contact angle measurements showed that the presence of multivalent ions in the injected brine is important for wettability alteration. Hence, the authors suggested that decreasing the concentration of ions in the brine is not the reason for the low salinity effect, but ion interaction with the surface of the carbonate is the key reason for the change in wettability of the surface.

Rashid et al (2015), performed contact angle measurements of an oil droplet on calcite substrate in the presence of brine containing a different composition of ions. Brine which contained only Na^+ and Cl^- ions did not affect the wettability of the surface at any concentration

(1000, 3000, and 5000 ppm). According to the results, significant wettability alteration towards water-wet was achieved only if brine contained Mg^{2+} . The most significant wettability alteration was achieved when brine contained only Mg^{2+} , Na^+ , and Cl^- . Presence of SO_4^{2-} was not necessary for wettability alteration. Although authors pointed out that sulfate ions can act as a catalyst during wettability alteration by Mg^{2+} and/or Ca^{2+} . The authors suggested mechanism for wettability alteration, where Mg^{2+} in brine reacts with CO_3^{2-} in precipitation reaction of $MgCO_3$. Carbonate ions come from the dissolution of $CaCO_3$. Since the dissolution of calcite at the surface was at equilibrium, depletion of CO_3^{2-} concentration will shift reaction equilibrium towards the right, to the production of Ca^{2+} and CO_3^{2-} , according to Le Chatelier's principle. Produced Ca^{2+} will react with carboxylic groups and desorb them from the surface according to the mechanism proposed by Strand et al (2008) rendering surface more water-wet. The authors also suggested that co-precipitation of $CaCO_3$ and $MgCO_3$ will change surface chemistry through the formation of dolomite.

2.4.3 Double layer expansion

According to this theory electrical double layer, which forms due to the difference of zeta potentials of oil-brine and rock-brine interfaces, is compressed due to the presence of ions in high saline water. At low salinities, the effect of ion screening is reduced and electrostatic repulsion between oil-brine and rock-brine interfaces is increased, therefore water film on rock surface expands and becomes more stable. This leads to a more water-wet condition of the surface. This was confirmed by Fathi, Austad, and Strand (2011), who reported that a decrease in the concentration of NaCl in seawater leads to additional oil recovery. According to the authors, as a concentration of Na^+ and Cl^- is higher in brine than other divalent ions, these monovalent ions form Stern layer on the charged rock surface which compresses double layer when the concentration of NaCl in injected brine is decreased divalent ions (Ca^{2+} , Mg^{2+} , and SO_4^{2-}) can interact with rock surface and contribute to double layer expansion.

2.4.4 Change of pH

Saikia, Mahadevan and Rao (2018) tested alternatives for sulfate ion which can cause serious fouling problems in the reservoir. In their research, they tested other sulfur oxyanions, namely bisulfites and metabisulfites. To supply these ions sodium bisulfite and sodium metabisulfite have been dissolved in brine. The addition of bisulfite and metabisulfite reduced contact angle between oil droplet and calcite surface. The addition of bisulfite changed contact angle within the first 10 seconds compared to 30 seconds which took for metabisulfite. For comparison

addition of sodium sulfate changed the contact angle only after 30 minutes. Also, it required a higher concentration of sodium sulfate to change the wettability of the surface, namely 3,000 ppm, compared to 80 and 360 ppm of bisulfite and metabisulfite, respectively. Besides, the authors proposed a mechanism for wettability alteration. According to their theory, the surface is least water-wet at isoelectric point (IEP). IEP is a point at which rock surface does not carry any charge and does not attract polar water molecules. IEP depends on the pH of the surrounding liquid. If pH gets further away from IEP, then the surface becomes charged and attracts polar molecules. Thus, the water-wetness of the surface increases as the charge of the surface increases. Since brine contains ions that can adsorb to the surface, the effect of brine composition on IEP should be accounted for to achieve desired wettability.

2.5 Modeling of LSWF

Omekeh et al (2012) made a simulation, which considers dissolution and multi-component ion exchange as a driving mechanism for improved oil recovery in carbonate rocks. In this model researchers considered the two-phase flow of water and oil, ions were included in the water phase. Na^+ , Ca^{2+} , Mg^{2+} , ions were modeled to exchange with a negative clay surface and adsorb to the surface, β_{Ca} , β_{Mg} are amounts of adsorbed Ca and Mg ions. To predict low salinity effect authors used relative permeability of oil and water phases as a function of desorption of divalent cations by using a weighing function, F.

$$k(S, \beta_{Ca}, \beta_{Mg}) = F(\beta_{Ca}, \beta_{Mg})k^{HS}(S) + (1 - F(\beta_{Ca}, \beta_{Mg}))k^{LS}(S) \quad (1)$$

where weighing function, F, is equal to:

$$F(\beta_{Ca}, \beta_{Mg}) = \frac{1}{1 + r m(\beta_{Ca}, \beta_{Mg})} \quad (2)$$

The model results were validated by history matching with laboratory results. The authors concluded that both dissolutions of minerals and ion exchange were responsible for improved oil recovery.

Qiao, Johns and Li (2016) in their work modeled LSW in chalk and limestone reservoirs. This was the first model of LSW which implemented both mineral dissolution and surface complexation reactions to predict oil recoveries. They used results from coreflooding experiments from Stevns Klint chalk and Middle Eastern carbonate cores. Surface complexation reactions were described by either an electrical diffusive layer model or a

nonelectrical diffusive layer model. If the change of surface potential was large, the electrical diffusive layer model was used. If otherwise, more simple to use a nonelectrical diffusive layer model. Authors used the following equation for predicting relative permeability:

$$k_{rw}^* = (1 - \theta)k_{rw,ww}^* + \theta k_{rw,ow}^* \quad (3)$$

$$k_{ro}^* = (1 - \theta)k_{ro,ww}^* + \theta k_{ro,ow}^* \quad (4)$$

where $k_{rw,ww}^*$, $k_{rw,ow}^*$, $k_{ro,ww}^*$, and $k_{ro,ow}^*$ are relative permeability values at the end-point oil-wet and end-point water-wet states. θ is the wettability indicator, which is represented by the following equation:

$$\theta = \frac{c - c_{ww}}{c_{ow} - c_{ww}} \quad (5)$$

where c , c_{ww} , and c_{ow} are concentrations of the carboxylic group on the surface of the rock at current, water-wet and oil-wet conditions, respectively. Saturation between endpoints was calculated from the Brooks-Corey model. Also, the model included the dissolution mechanism represented by transition state theory rate law. The transition state theory assumes that there is an intermediate state between reactants and products of chemical reaction. Oil recovery and effluent concentrations predicted by simulation matched the experimental measurements.

2.6 Molecular dynamics simulations of low salinity waterflooding

The lack of understanding of molecularly interpreted studies at solid/brine and brine/oil interfaces leads researchers to seek other methods to explain wettability alteration during LSW. One of such methods is the MDS. The molecular dynamics simulations allow gaining fundamental insight into the mechanism responsible for wettability alteration during LSW. (Khanamiri et al, 2014; Koleini et al, 2018; Zhao et al, 2018). By using MDS one can provide a comprehensive understanding of the properties of the molecules. The MDS is used here to evaluate the equilibrium and transport properties of the complex systems, which cannot be calculated analytically. The atomic-level properties can be linked with macroscopic properties by thermodynamics and statistical mechanics. One of the drawbacks of MDS studies is that it cannot model the reactions, therefore with current technology it is not possible to model dissolution of rock at a molecular level. All of the studies, including the current one, do not take the dissolution/precipitation mechanism into account when modeling LSW.

Koleini et al (2018) used MDS to better understand molecular interactions on the calcite-brine interface. In their study, they have simulated brine films with different ions over a calcite slab. Two brine films were tested in their work: low saline seawater (SW) and high saline formation water (FW). Pair correlation function analysis revealed that water molecules adsorb to the surface of the rock and form monolayer with density twice large than bulk water density. The density of the monolayer is larger in FW than in SW. Authors argued that this dense monolayer acts as a barrier between rock surface and potentially wettability altering ions such as SO_4^{2-} . On the contrary, a smaller density of water monolayer formed in brine with lower salinity grants easier access to active ions which in turn can contribute to wettability alteration. Another result that was noticed from their work was that there exists an interaction between Na^+ ions and calcite surface which keeps the Na^+ ions attached to the negative sites on the surface, though these ions do not directly interact with the rock surface due to the presence of H_2O monolayer. It was shown that the concentration of Na^+ ions at the interface is greater with low saline brine than with high saline brine. After this layer comes the brine layer which is rich in anions like Cl^- and SO_4^{2-} . The latter two layers form an electrical double layer. Positively charged Na^+ ions form the Stern layer, while brine film rich in anions forms a diffuse layer. The overall charge at the edge of the diffuse layer was negative in SW, while in FW charge at the endpoint of the diffuse layer was positive. The authors explained it by a higher concentration of sulfate ions in SW than in FW. This finding matched with the experimental results which demonstrated the same result by measuring the zeta potential of limestone minerals. (Alotaibi et al, 2017).

Zhao et al (2018) performed MDS on both charged and neutral surfaces of the calcite. The charged surface was obtained by cleaving the calcite mineral at $\{0\ 0\ 0\ 1\}$ cleavage plane, whereas neutral surface was obtained at $\{1\ 0\ 1\ 4\}$ cleavage plane. The neutral surface is obtained because Ca and CO_3 are located in the alternating arrangement in the same layer. Positive and negative charges developed by Ca and oxygen atoms in carbonate cancel each other, thus creating a neutral surface. The charged surface is obtained because $\{0\ 0\ 0\ 1\}$ cleavage plane results in the surface layer which is rich in either Ca or CO_3 , thus creating positively or negatively charged surface. The authors used decane to represent the crude oil and different concentrations of Na^+ and Cl^- (0.2 M, 0.5 M, and 1M) in brine were tested. In all of their simulations authors have placed liquids between two calcite slabs to represent the behavior of molecules inside nanopores. The initial configuration of molecules is given in Figure 3.

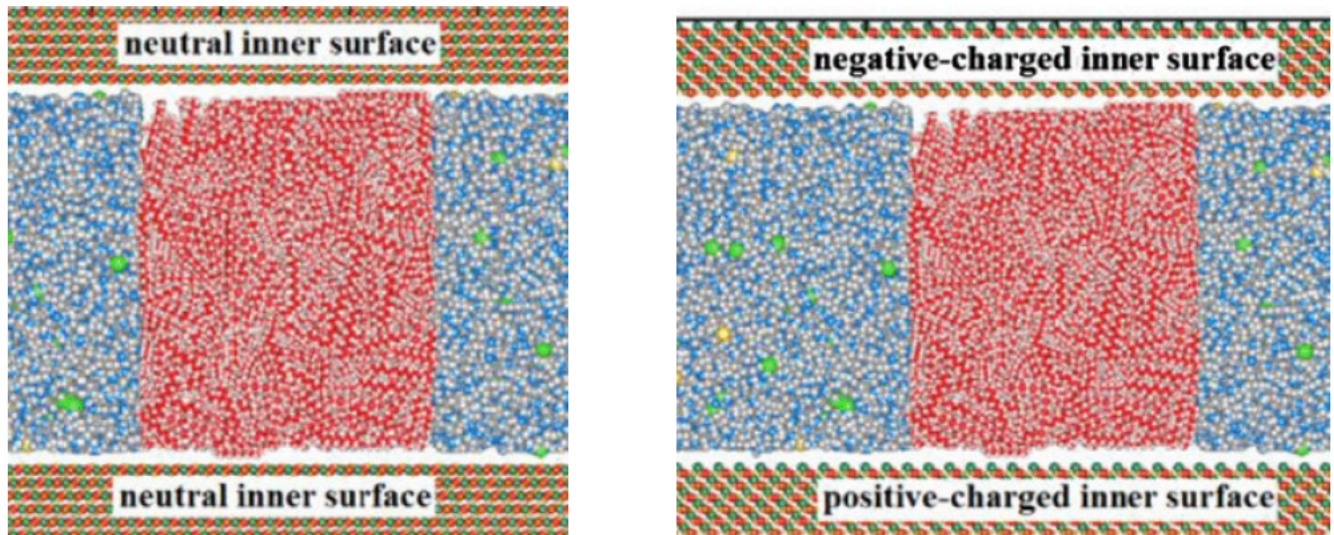


Figure 3. Illustration of simulation structure developed by Zhao et al (2018)

The results showed that charged surfaces create a strong electrostatic field that separated Na^+ and Cl^- ions. Positive ions were absorbed by the negative surface and negative ions were absorbed by the positive surface. The neutral surface of calcite showed no affinity to the absorption of ions. For both surfaces, structured water molecules were observed near the surfaces of the rock. Alteration of the salinity had less effect on the wettability of the neutral surface compared to the charged surface. The charged surface showed higher sensitivity to salinity. At low salinities, charged surface showed higher affinity towards decane molecules, whereas high salinity, 1M, resulting in the completely water-wet surface as can be seen from Figure 4. Contrary to this, change in salinity did not affect the distribution of decane molecules on the neutral surface as can be seen from Figure 5.

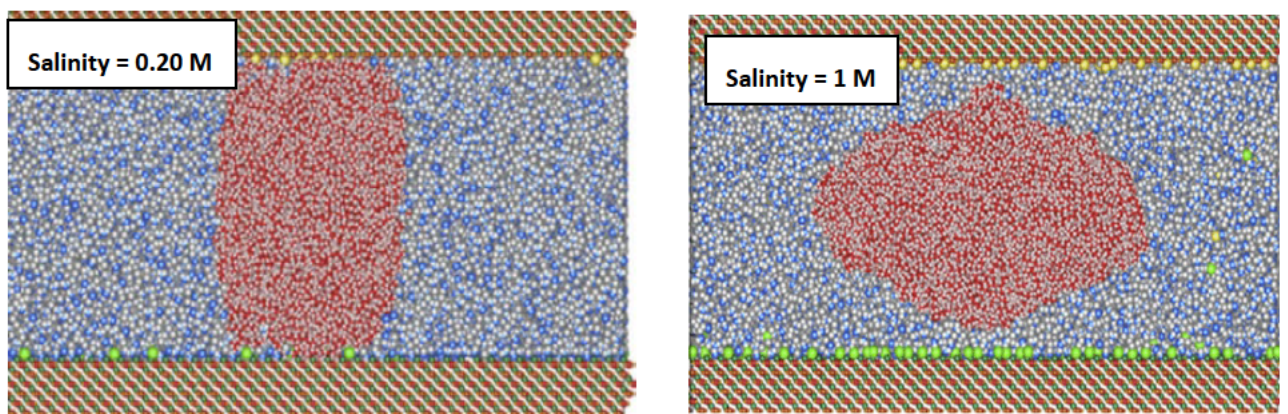


Figure 4. Distribution of molecules after equilibration, charged inner surface (Zhao et al, 2018)

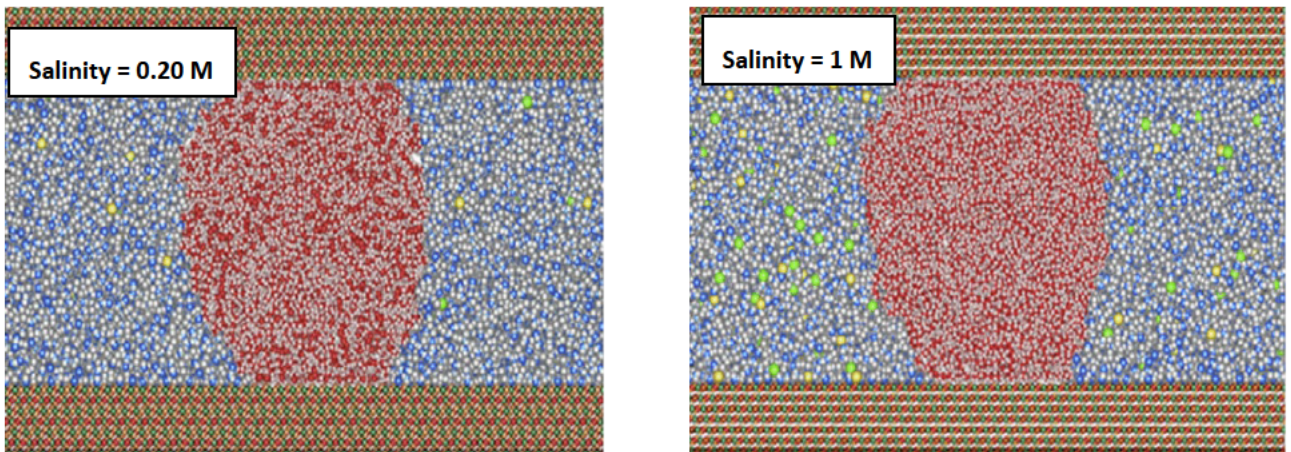


Figure 5. Distribution of molecules after equilibration neutral inner surfaces (Zhao et al, 2018)

The study performed by Chang et al studied the wettability of water and oil on different rock surfaces, one of the rocks was calcite cleaved along the $\{1\ 0\ 0\}$ plane. The study simulated the behavior of the water droplet in the oil phase placed on the rock surface. Different oil phase constituents were tested. Among the tested chemicals in the oil phase were: hexane, dodecane, thiophene, toluene, and pyridine. It was shown that a particular cleavage plane of calcite mineral results in the strongly water-wet surface as can be seen from Figure 6. The interaction energy between rock and water was much higher compared to interaction energy between rock and oil. Also, researchers demonstrated that wettability of the rock depends on the constituents of the oil phase. More polar chemicals in the oil phase resulted in the less water-wet surface. This can be explained by the fact that polar components are attracted to the charged surface and compete with water molecules for charged surface sites. Interaction energy calculations showed that polar oil molecules exhibit stronger attraction towards rock surfaces compared to water molecules. Whereas, polar oil molecules have less interaction energy with rock compared to the interaction energy of water with rock.

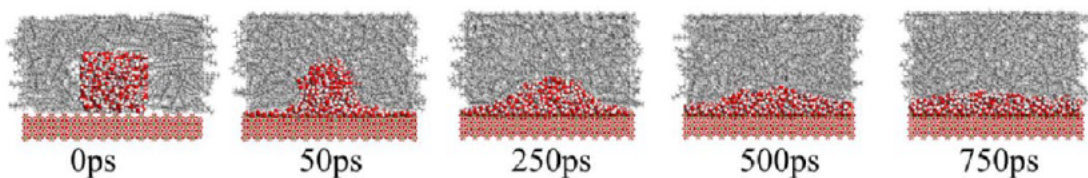


Figure 6. Behavior of water droplet on the calcite surface. (Chang et al, 2018)

Greathouse et al (2017) used MDS to assess the mechanisms of low salinity effect by modeling adsorption of representative organic molecules onto the rock surface. They have studied the molecular structure, binding energy, and interfacial behavior of saturate, aromatic and resin molecules near the rock surface. The rock surface studied was basal surfaces of

various clay minerals. The authors analyzed the effect of aqueous cations at the rock/fluid interface on the adsorption of organic molecules onto the rock surface. The study of cation-organic complexes revealed that organic anions strongly coordinate with Ca^{2+} rather than Na^+ . The results demonstrated that cation bridging enhances the adsorption of organic complexes onto the surface, especially when the organic molecule has carboxylate group or aromatic π electrons of toluene, which strongly interact with charged cations.

In a study performed by Mehana and Fahes (2018), the interaction between clay surface and water with varying concentrations of Na^+ , Cl^- , and Ca^{2+} were studied by MDS. The estimations of brine film and calculations of interaction energy showed shrinkage of the electric double layer in low salinity brine. The shrinkage of the electrical double layer on clay surfaces contradicts the assumption of the EDL mechanism. It was observed that the behavior of monovalent and divalent ion did not differ from each other.

Khanamiri et al (2014) conducted molecular dynamics simulation of a system consisting of the rock surface, brine, and acetic acid. The acetic acid was used to model the behavior of polar components in the oil. The brine included sodium and calcium chloride ions. The rock used in simulations was basal kaolinite. The results showed that acetic acid was initially strongly adhered to the rock surface by hydrogen bonds. The density profile of acetic acid molecules demonstrated higher desorption of polar organic components at lower salinities. Also, results demonstrated the expansion of the electrical double layer in the low salinity model.

Effect of ions in the aqueous phase on the aggregation of polar components in the oil was studied in the paper performed by Tirjoo et al (2018). It was observed that Na^+ , Mg^{2+} and Ca^{2+} ions have ascending, descending and ascending trend, respectively, on sedimentation of polar organic components. Electronegative sites in the structure of organic component can adsorb ions and increase adherence of the molecule onto the rock surface.

3. Molecular Dynamics Simulation

3.1 Basics of molecular dynamics simulation

In MDS, an atom is represented as a point which has mass and charge. The motion of the atoms can be calculated by using Newtonian dynamics to determine the net force and acceleration of each atom. The net force acting on each atom is derived from potential energy function. Therefore, proper MDS requires accurate force field parameters which describe the classical potential energy functions between the particles present in the system. The forces acting on particles can be divided into two types: bonding and non-bonding.

3.1.1 Bonding interaction

The bonding interactions include forces acting at the intramolecular level. The potential function of the bonding interactions is:

$$E_{intramolecular} = E_{bond} + E_{angle} + E_{torsion} = \frac{1}{2} \sum_{bonds} k_r (r_{ij} - r_0)^2 + \frac{1}{2} \sum_{angles} k_\theta (\theta_{ijl} - \theta_0)^2 + \frac{1}{2} \sum_{torsion} \sum_m k_{\phi,m} (1 + \cos(m\phi_{ijkl} - \gamma_m))^2 \quad (6)$$

where E_{bond} , E_{angle} , and $E_{torsion}$ are the bond strength potential, bond angle potential, and bond torsion potential, respectively. In the above equation k_r , k_θ , k_ϕ , r_{ij} , r_0 , θ_{ijl} , θ_0 , ϕ_{ijkl} and γ_m represent stiffness parameter for the bond, stiffness parameter for an angle, dihedral stiffness, bond length, equilibrium length of the bond, the angle between two bonds, equilibrium angle between two bonds, the angle between two intersecting planes, and equilibrium angle between two planes, respectively. The first term in the equation (6) calculates the interaction between a pair of bonded atoms, it is modeled as a harmonic potential that results in growth in energy as length, r_{ij} , deviates from the reference value, r_0 . The second term calculates the angle between three atoms and again modeled as harmonic potential. The third term is responsible for calculating the torsional potential, which estimates how energy changes when a bond rotates.

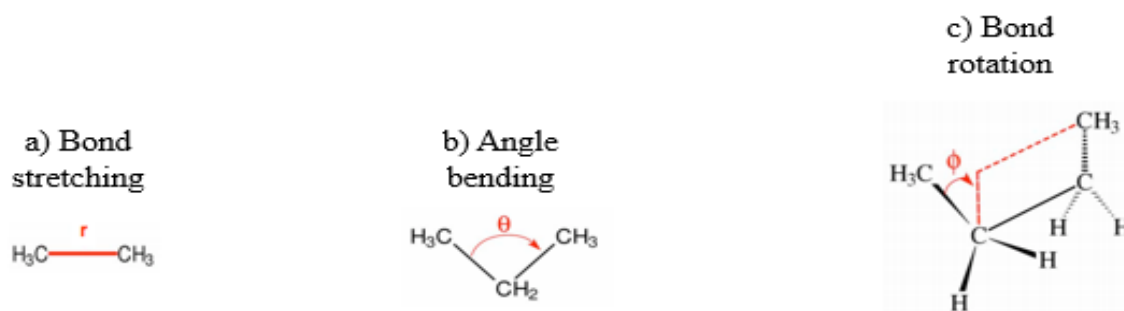


Figure 7. Schematic representation of bonding contribution to molecular mechanics: a) bond stretching, b) angle bending, and c) bond rotation.

3.1.2 *Van der Waals interaction*

Two types of non-bonding interactions are usually considered: electrostatic interaction and van der Waals interactions. Since non-bonding interactions do not depend on the bonding relationship between atoms, they are usually represented as a function of distance. Van der Waals force is a short-range force between two particles induced by oscillations of the orbital electrons. The most common model used to describe van der Waals interactions is Lennard-Jones interaction potential. The expression which describes Lennard-Jones potential is as follows:

$$E_{LJ} = 4\varepsilon \left[\left(\frac{\sigma}{r} \right)^{12} - \left(\frac{\sigma}{r} \right)^6 \right] \quad (7)$$

where ε is the constant which describes the strength of interaction, σ is the distance between two particles at which potential is equal to 0. When the distance between two particles is larger than σ , then the interaction is attractive, at closer distances the interaction is repulsive. Since van der Waals is negligible over large distances, usually cut-off distance is introduced for computational convenience. The cut-off distance, r_c , usually is derived as $r_c = 2.5\sigma$.

3.1.3 *Electrostatic interaction*

Another important non-bonding interaction is the interaction between electrically charged particles. The most common model to describe this interaction is the Coulomb potential model. The expression for the Coulomb potential model is as follows:

$$E_C(r) = \frac{q_1 q_2}{4\pi\varepsilon_0 r} \quad (8)$$

where q is the charge of the particle, ϵ_0 is the permittivity of the medium in which charged particles are immersed in. Compared to van der Waals interaction, the Coulomb forces are significant over large distances. Therefore, the model requires the most computational power compared to other models in molecular dynamics.

3.1.4 Periodic boundary

Since in MD simulations few molecules are used to represent bulk properties of the system, it is important to take into account boundary effects. For a small simulation box with few atoms, most atoms would be affected by boundary, which will distort the bulk properties of the system. Therefore periodic boundary conditions are used in MD simulations to exclude boundary effects and simulate atoms as if they were in the bulk fluid. In periodic boundary conditions, imaginary copies of the simulation box are projected next to the original simulation box. Thus, the original simulation box would be surrounded by 26 other identical boxes. Coordinates in imaginary boxes are derived by the addition or subtraction of integral multiples of the box sides. If a particle leaves the box from one edge of the box, an imaginary particle enters the box from the opposite edge of the box. Therefore, the number of atoms in the original box does not change (Figure 7). A simulation box of different shapes can be applied to better suit the particular system. The most widely used shapes are cube, parallelepiped, and truncated octahedron. Later one is used for creating periodic cells that are approximately spherical and ideal for the simulation of spherical molecules.

When using a periodic boundary condition, it is important to choose an appropriate cut-off distance for van der Waal's interaction. If cell size is small compared to the cut off distance, then particles may interact with its image or interact with the same molecule twice, creating disturbances in the system. Therefore, cutoff distance cannot be larger than half the length of the shortest side of the cell. For long-range interactions it is impossible to prevent such situations, therefore long-range order will be imposed upon the system. Applicability of periodic boundary can be assessed empirically by analyzing the results of simulations done with different cell sizes and shapes.

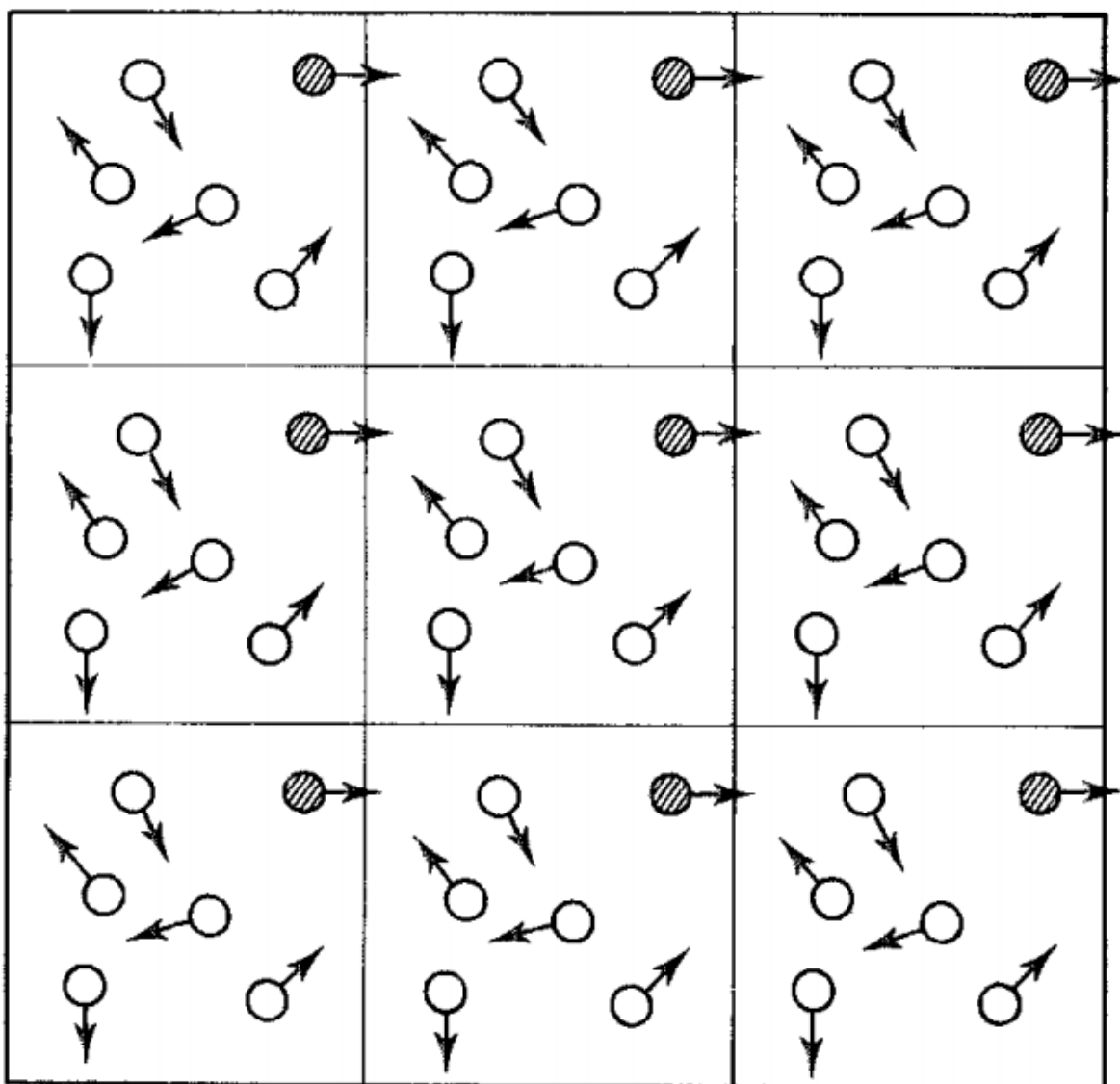


Figure 7. Schematic representation of periodic cells for a cubic system in two dimensions (Leach, 2001)

3.1.5 *Simulation time step*

Choosing an appropriate time step for simulation is important to preserve energy and momentum conservation of the system and to prevent numerical overflow, which will result in failure of the simulation. If the time step is too small than it would require more computational power to cover the whole phase space. Too large time step results in high energy overlaps between atoms which will create instabilities in the integration algorithm. (Figure 8)

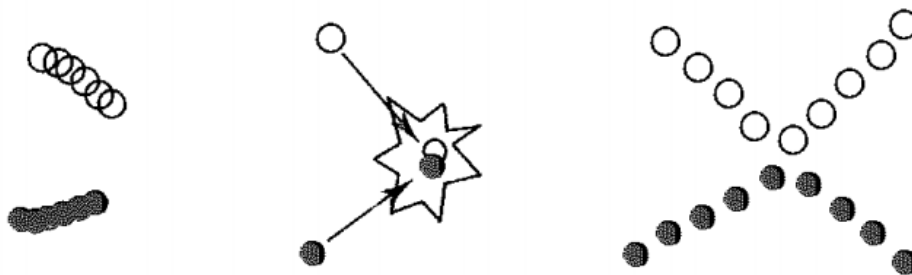


Figure 8. Graphical representation of collision simulation between two atoms by using different time steps. Small time step (left), large time step (center), appropriate time step (right). (Leach, 2001)

When choosing a time step for simulation of fluid it is crucial to make time step smaller compared to the mean time between collisions of particles. If flexible molecules are present in the system, then the general rule of thumb is to take time step ten times smaller than the time of the shortest period of motion. For flexible molecules like long-chain alkanes, which are used in this work, bond stretches cause the highest-frequency vibrations, especially those of bonds of hydrogen atoms. The repeat period of vibration of a C-H bond is approximately 10 fs. Taking this into account, the time step of 1 fs should be appropriate to simulate the system in this project.

The fact that time step must be ten times smaller than the shortest motion creates major restriction, these high-frequency motions, like bond vibrations, are of little interest since they do not contribute to the conformational changes in the system. Therefore, one can increase the time step without compromising the accuracy of the simulation by constraining the individual internal coordinates without affecting other internal degrees of freedom.

3.1.6 *Radial distribution functions*

The radial distribution function is used to describe the configuration of particles in the system. The most common radial distribution function used is the pair distribution function, $g(r)$. $g(r)$ gives the probability of finding a particle (atom or molecule) at distance r from another particle compared to the ideal gas distribution. Therefore, the values of $g(r)$ are dimensionless.

Higher-order radial distribution functions, like triplet radial distribution functions, do exist, but in this paper, radial distribution function refers to the pairwise version. In a crystalline structure, radial distribution function has an infinite number of peaks at different separations and heights, which describe properties of the lattice cell. In liquids, the radial distribution function is characterized by a few numbers of peaks at short distances which slowly decay at a

constant value at large distances. The typical radial distribution function of a liquid is given in Figure 9.

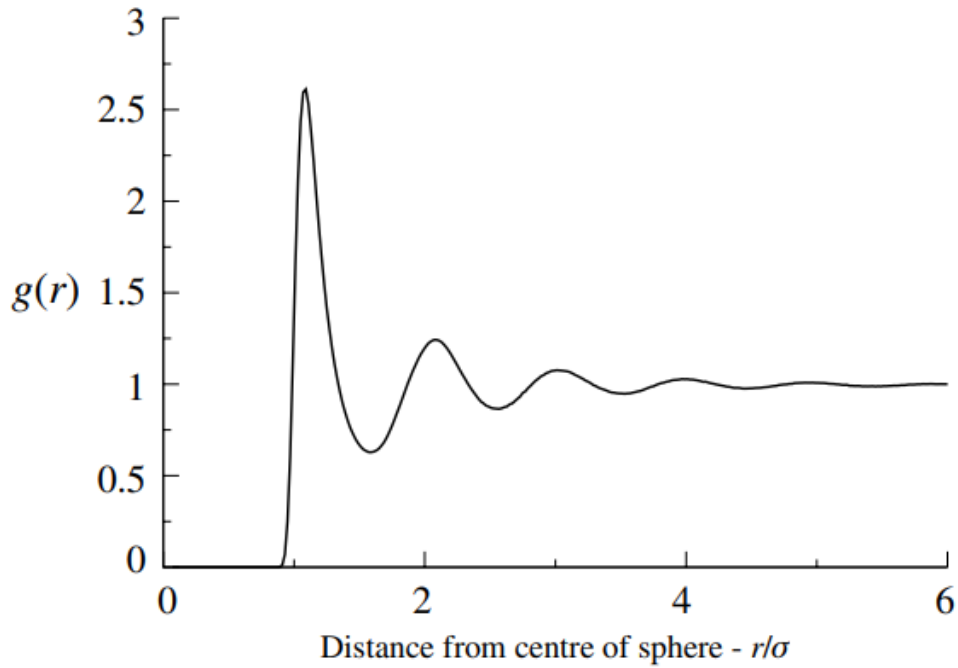


Figure 9. Radial distribution function derived from the MDS of liquid argon (Barrat and Hansen, 2003)

$g(r)$ is calculated by sorting neighbors around each particle into distance bins or histograms. The number of neighbor particles is then averaged over the entire simulation cell.

3.1.7 Interaction energy

The interaction energy between liquid molecules and rock surfaces can be used to quantitatively evaluate the interaction between aqueous/oleic phase and surface. The interaction energy between water molecules and calcite molecules can be calculated by the following equation:

$$E_{W-c} = E_{W+c} - E_W - E_C \quad (9)$$

where E_W is the total energy of water molecules, E_C is the total energy of calcite molecules, E_{W-c} is the total energy of a system containing only water and calcite molecules. The total energy of the system includes all bonding energies, van der Waals interaction energy, and electrostatic interaction energy. The interaction energy between molecules in the oleic phase and calcite molecules can be described by the following equation:

$$E_{O-c} = E_{O+c} - E_O - E_C \quad (10)$$

where E_O is the total energy of water molecules, E_C is the total energy of calcite molecules, E_{O-C} is the total energy of a system containing only oil and calcite molecules. Difference between interaction energies, E_{W-C} and E_{O-C} , is determined by the following equation:

$$DE = E_{W-C} - E_{O-C} \quad (11)$$

3.2 Simulation parameters

The simulation will be run in a box with dimensions $2.5 \times 2.5 \times 8 \text{ nm}$. Rock consists of calcite molecules. The crystal structure is 5 atomic layers thick in z-dimension, which will give rock surface 15 Angstrom thick. The calcite crystal was cleaved along the (1014) plane. At this cleavage surface, Ca^{2+} and CO_3^{2-} are located in the same layer, which creates neutral surface due to the alternating arrangement of the oppositely charged ions. The illustration of the calcite slab is given in Figure 10 and Figure 11.

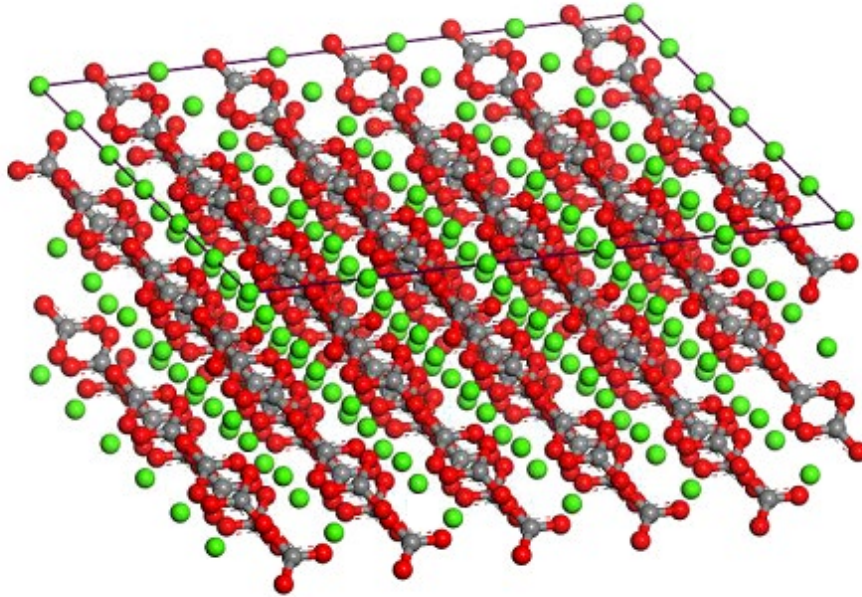


Figure 10. 3D illustration of calcite crystal. (green: calcite, red: oxygen, grey: carbon)

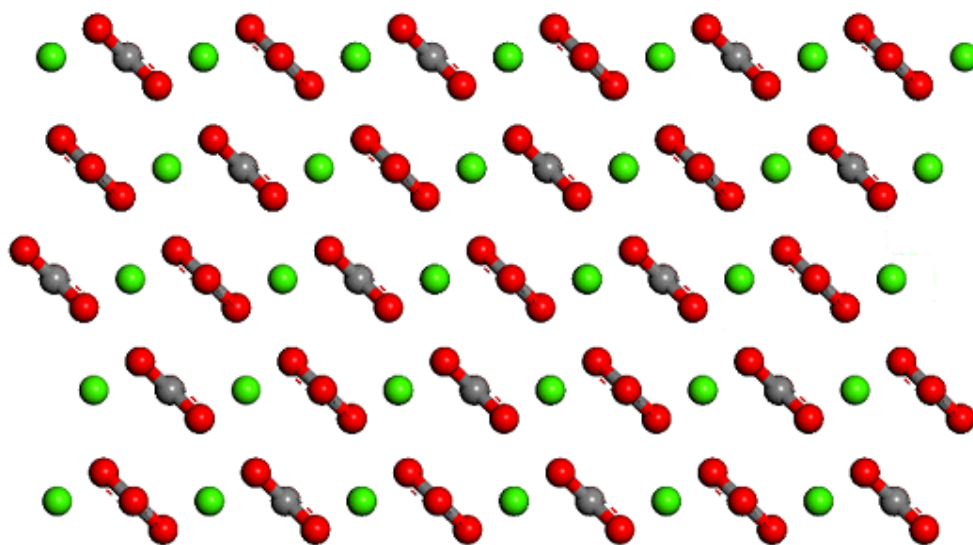


Figure 11. Side view of calcite crystal

The aqueous layer consists of 250 H₂O molecules. Different amounts of Na⁺, Cl⁻, Ca²⁺, Mg²⁺, and SO₄²⁻ ions will be dissolved in water. Multiple simulations, which have different ion concentrations in the aqueous phase, will be run to check the stability brine film. Simulations will be done for deionized water (DIW), low salinity brine (LS), and high salinity brine (HS). The brine compositions are given in Table 1. At first DIW water was studied, then monovalent ions (Na⁺ and Cl⁻) were added to the DIW to obtain LS and investigate their effect on brine film thickness. After that, divalent ions (Mg²⁺, Ca²⁺, and SO₄²⁻) were added to LS to obtain HS and investigate the effect of divalent cations on brine film. The oil phase contains 64 molecules of n-decane. 4 molecules of heptanoic acid will be dissolved in decane to represent the polar components in the crude oil. For an illustration of molecules used, refer to Figure 12. The initial configuration of molecules before equilibration is given in Figure 13. The 3 consecutive layers of rock, water, and oil were topped by another water, rock layers to minimize periodic boundary effect in the z-direction.

Table 1. Number of ions dissolved in the aqueous phase for three cases studied

Ion	DIW	LS	HS
Na ⁺	0	2	7
Cl ⁻	0	2	7
Mg ²⁺	0	0	2
Ca ²⁺	0	0	2
SO ₄ ²⁻	0	0	2
Salinity (ppm)	0	21,000	131,000

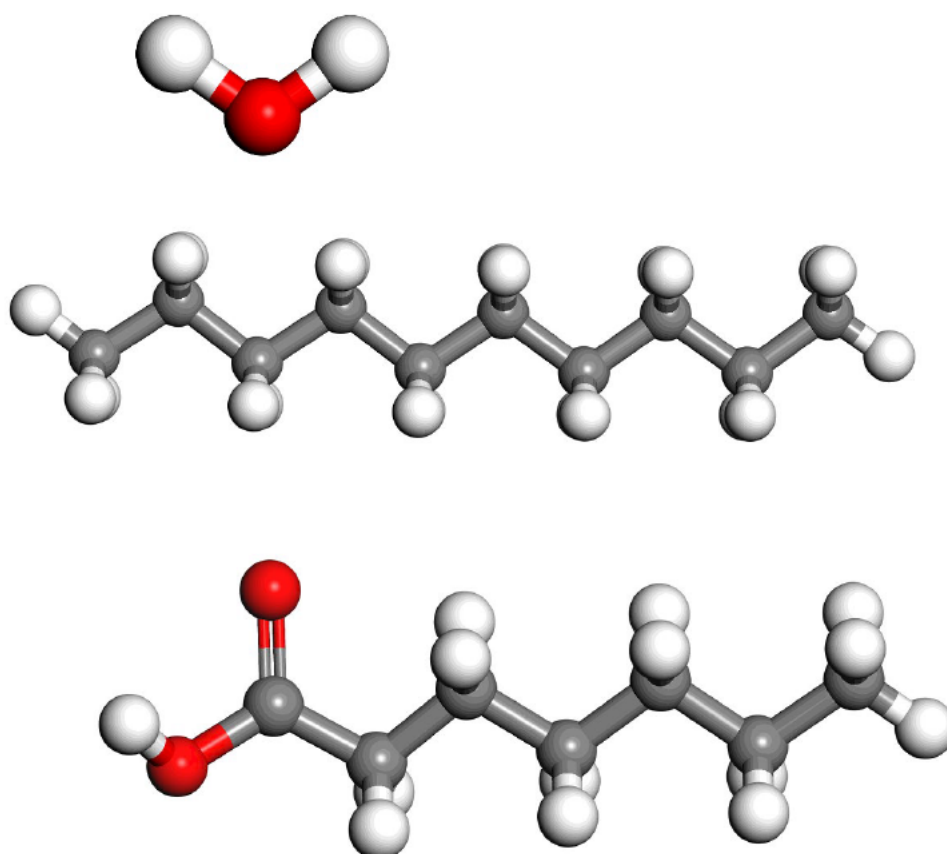


Figure 12. Illustration of molecules used in simulation: water, decane and heptanoic acid. (from top to bottom) (white: hydrogen, red: oxygen, grey: carbon)

The models were constructed and computational results were obtained using software programs from Dassault Systèmes BIOVIA. The force-field-based molecular dynamics simulations were performed with the Forcite module, and graphical displays were generated with BIOVIA Materials Studio. During the MD simulation coordinates of the rock atoms were

fixed, while atoms in brine and oil phases were relaxed. GEOMOPT module was used to optimize the initial structure of the system. It was observed that simulations 2 ns long are enough to make the model reach a stable state. The canonical ensemble NVT was adopted in all simulations. Andersen thermostat was used to keep the temperature at 298 K. Van der Waals interactions were calculated by using the atom-based method and cutoff distance of 12.5 Angstrom was used to minimize computational requirements. Electrostatic interactions were determined by the Ewald method. Timestep of 1 fs was used for all simulations and trajectory results were recorded every 500 ps.

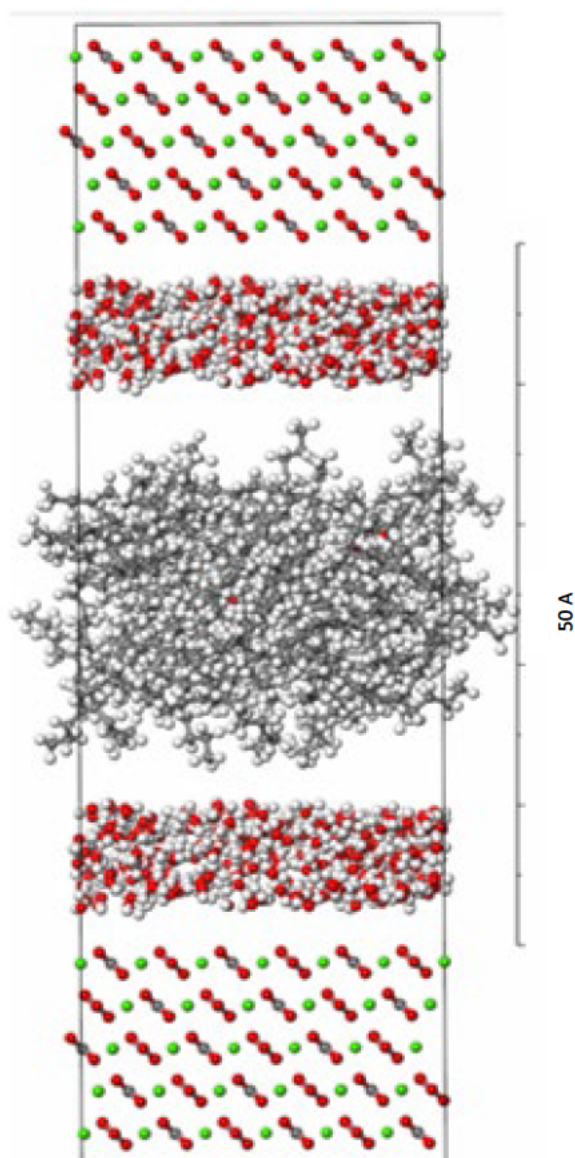


Figure 13. Initial configuration of the simulation cell with deionized water

Molecular interaction between atoms was described by the Condensed-phase Optimized Molecular Potential for Atomistic Simulation Studies (COMPASS) forcefield (Sun, 1998). The COMPASS forcefield covers the structural, conformational, vibrational and thermophysical properties of molecules that are of interest to this work. The COMPASS is the ab initio forcefield, which means that parameters for the molecules were derived from first principles and then optimized to fit the experimental results. The wide range of molecules covered by the COMPASS forcefield allows studying interfacial systems, which of interest for this paper. The major drawback of this forcefield is the fact that it cannot model bonded interactions between two phases. Therefore, it must be assumed that only non-bonded interactions exist between the two phases.

4. Results and Discussion

5.1 Initial equilibration

The simulation cell configurations after the energy minimization process are given in Figure 14. Energy minimization for 500 steps was considered to be sufficient to obtain the equilibrated system. This was confirmed by running the simulation for an additional 200 steps, which did not result in significant changes in parameters of the systems. The calculated total energies of the system at different optimizations steps are given in Figure 15. As can be seen from the figures total energies level out after 500 steps of energy optimization meaning that the system reached equilibrated condition.

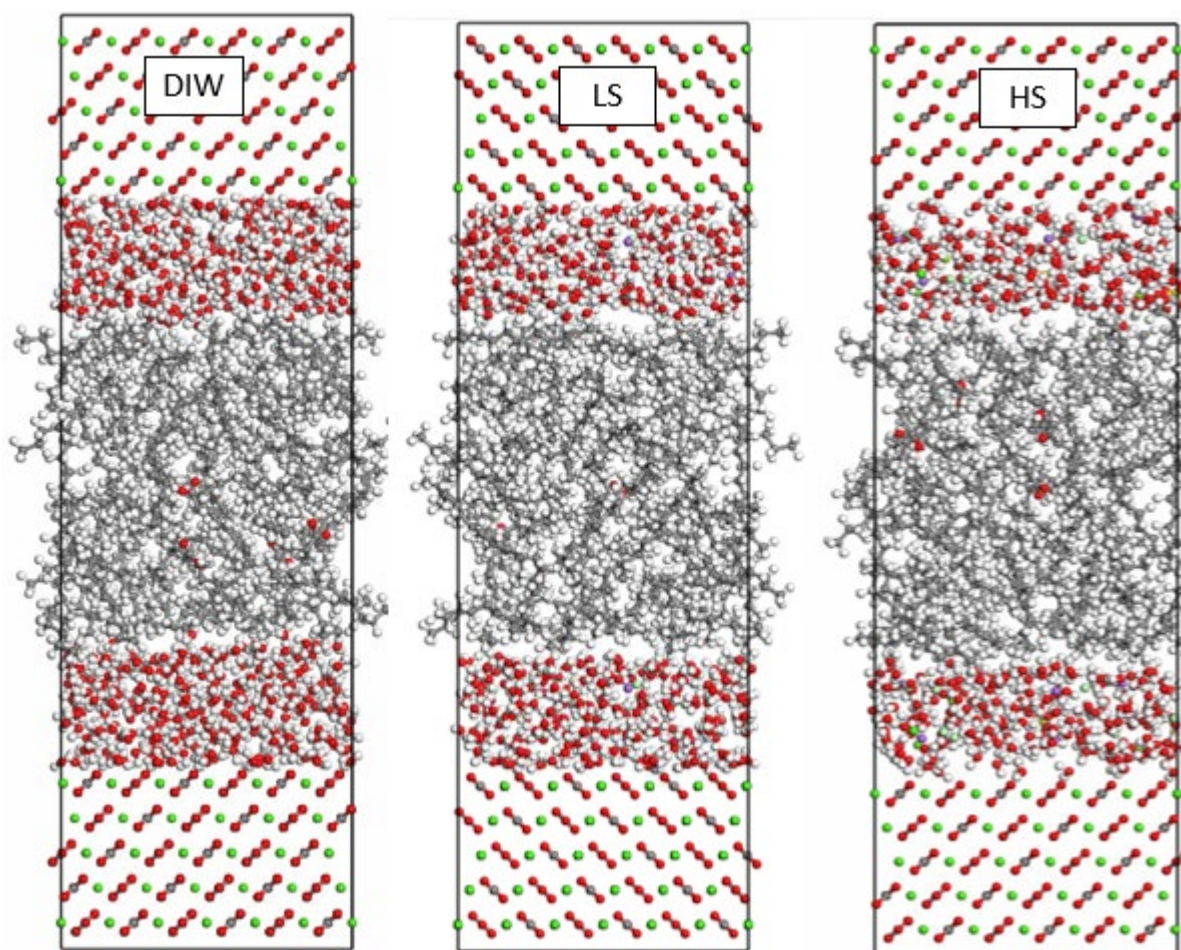


Figure 14. Snapshots of the simulation cells after energy minimization (pale green: chlorine, violet: sodium, yellow: sulfur, olive: magnesium)

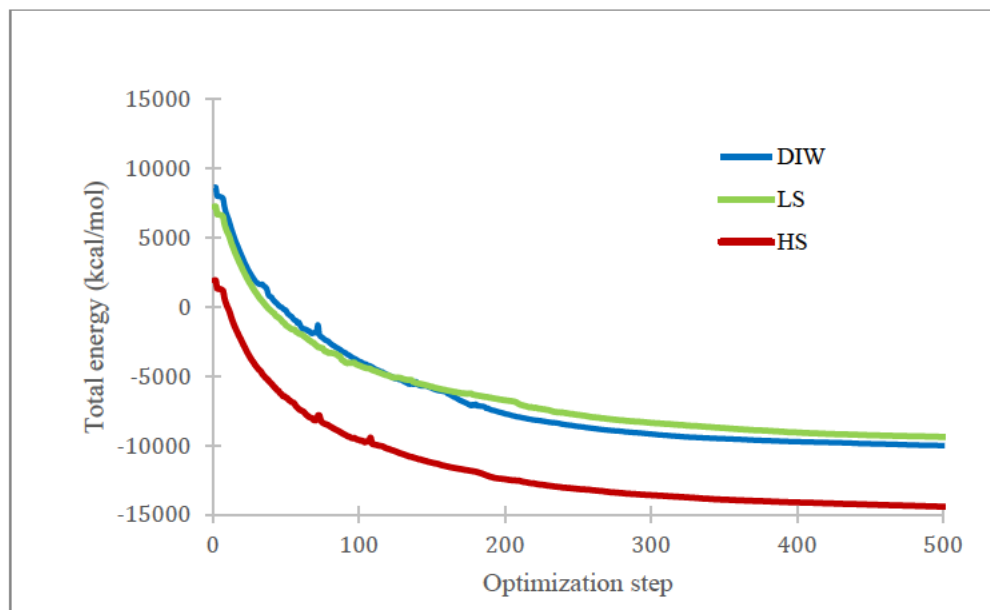


Figure 15. The total energy of the DIW case at different energy optimization step

5.2 Radial distribution function

The radial distribution function between water and calcite molecules given in Figure 16. At short distances (less than atomic diameter) $g(r)$ is equal to 0, due to the strong van der Waal repulsive forces. The first peak occurs at a distance of 1.4 Å, which indicates the first layer of adsorption fully consisting of water molecules. This agrees with the findings of Koleini et al (2018). The RDF profile of water molecules indicates the formation of three hydration layers of water molecules in the first 4 Å, which is in agreement with experimental and simulation results (Fenter et al, 2013; Kerisit and Parker, 2004; Ricci et al, 2013; Zhu, Xu and Tang, 2013). The second hydration layer of water molecules is at 2.3 Å, the third adsorption layer is centered at approximately at 2.9 Å. Also, one can observe that $g(r)$ is higher for the case with high salinity brine, which indicates a higher density of water molecules at higher salinities.

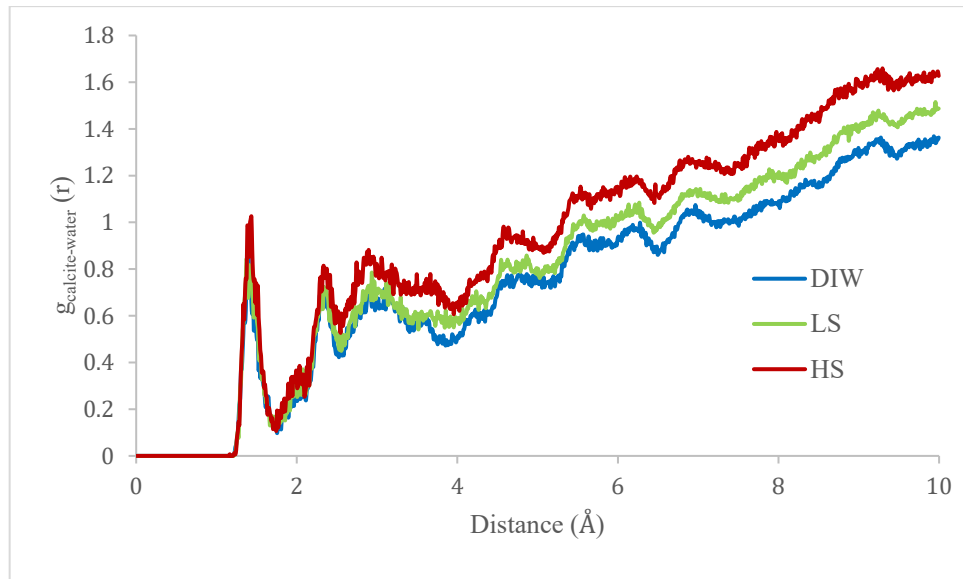


Figure 16. Radial distribution function between calcite and water molecules

5.3 Brine thickness

By using the relative concentration profile of water molecules one can determine the thickness of the water layer. The concentration profile of the chemicals studied here is calculated by dividing the system into 100 bins along the z-direction and estimating the concentration in each bin. As can be seen from relative concentration profiles given in Figure 17, the thickness of the water layer decreases with an increase in salinity of the brine. The thickness of the deionized water layer was 14.7 Å, the thickness of low salinity brine was 13.5 Å and the thickness of high salinity brine was equal to 11.2 Å.

Also, one can observe that the relative concentration in the first three hydration layers of water layer are larger for high salinity case and the height of the peaks decreases as the salinity of the brine decreases. Therefore, one can conclude that water molecules are more arranged for the DIW case. The order of arrangement decreases as the number of ions dissolved in water increases.

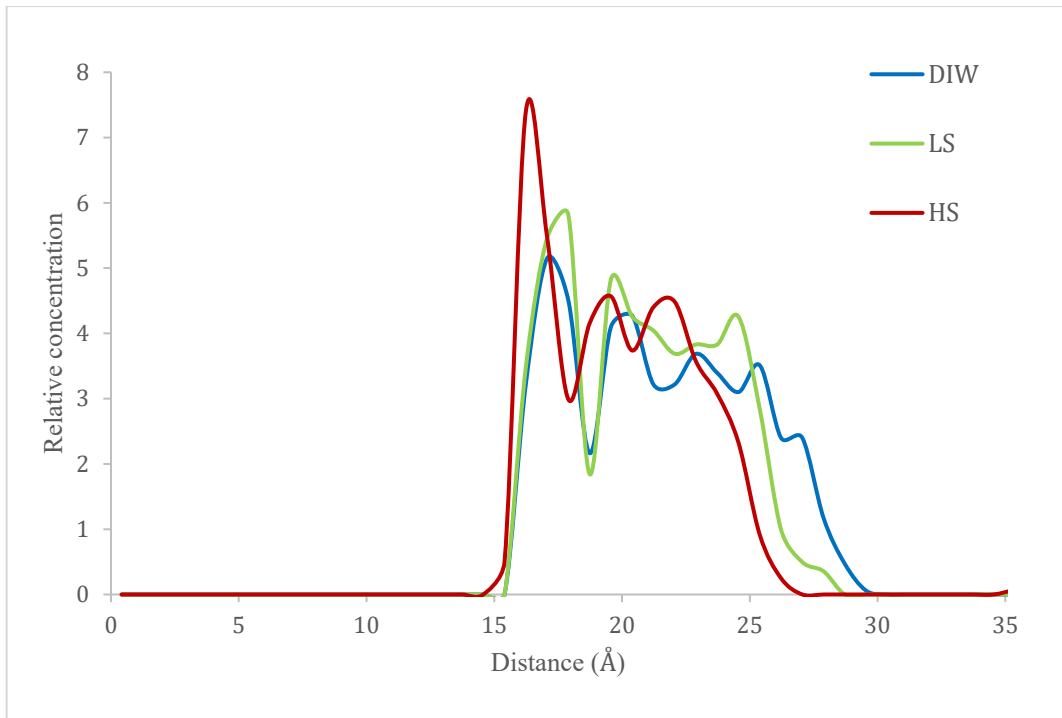
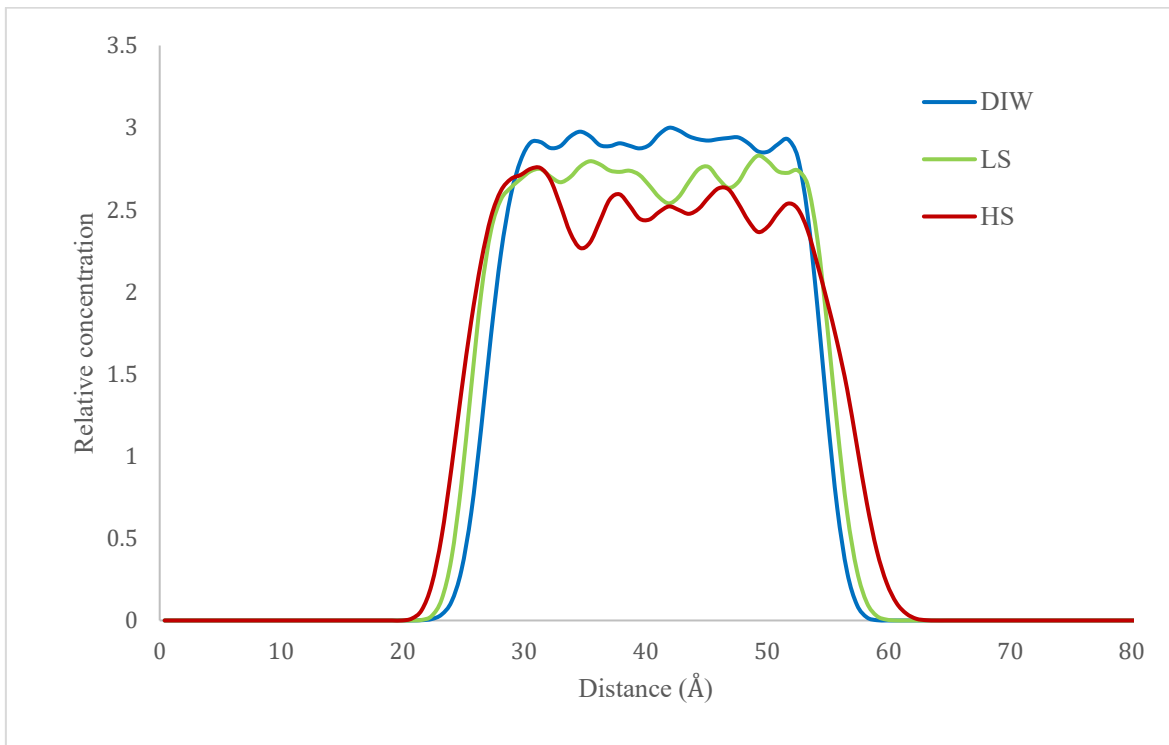


Figure 17. Relative concentration profile of water molecules

The relative concentration profile of oil molecules confirms the results derived from the previous graph. As can be seen from Figure 18, as the salinity of brine decreases, the thickness of the oil layer shrinks due to the expansion of the water layer.



5.4 Distribution of ions in the brine

From the radial distribution function between rock and water, we observed that the first adsorption layer on the rock surface consists of a water monolayer at a distance of 1.4 Å (Figure 16). For HS brine the second adsorption layer contains mainly Na⁺ ions and is located at a distance of 2 Å from the rock surface (Figure 19). The Na⁺ ions located in the second adsorption layer do not directly interact with the rock surface due to the presence of the first water layer strongly adhered to the rock surface. The relative concentration profile of Na⁺ ions indicates that these ions are mainly distributed at the interface between brine and rock rather than the bulk of the brine phase.

The third adsorption layer consists of SO₄²⁻ and Cl⁻, (Figures 19). The appearance of anions, like SO₄²⁻ and Cl⁻, can be explained by specific charge distribution of calcite surface, which allows attractive electrostatic forces between positive sites on the surface of the rock and negative ions in the brine (Ricci et al 2013). This allows adsorption of sulfate ions on the calcite surface, which can explain the positive effect of sulfate ions on additional oil recovery during low salinity waterflooding (Karimi et al, 2016; Tabrizy, Hamouda and Denoyel, 2011). According to this fact, adsorption of sulfate ions onto the surface contributes to the release of previously adsorbed fatty acids.

The second adsorption layer in HS brine, which consists of Na⁺ ions, can be regarded as a positive Stern layer, whereas the third adsorption layer, which mainly consists of anions, can be regarded as a negative diffuse layer. Shrinkage of water layer in HS brine can be explained by electrostatic attraction between these two layers. The Ca²⁺ and Mg²⁺ ions were mainly distributed in the bulk of brine rather than at the interface (Figure 19). This result agrees with the study performed by Chen, Panagiotopoulos and Giannelis (2015), who found out that magnesium and calcium ions have the least effect on improving oil recovery. This can be explained by a larger hydration shell of divalent cations and their larger positive charge.

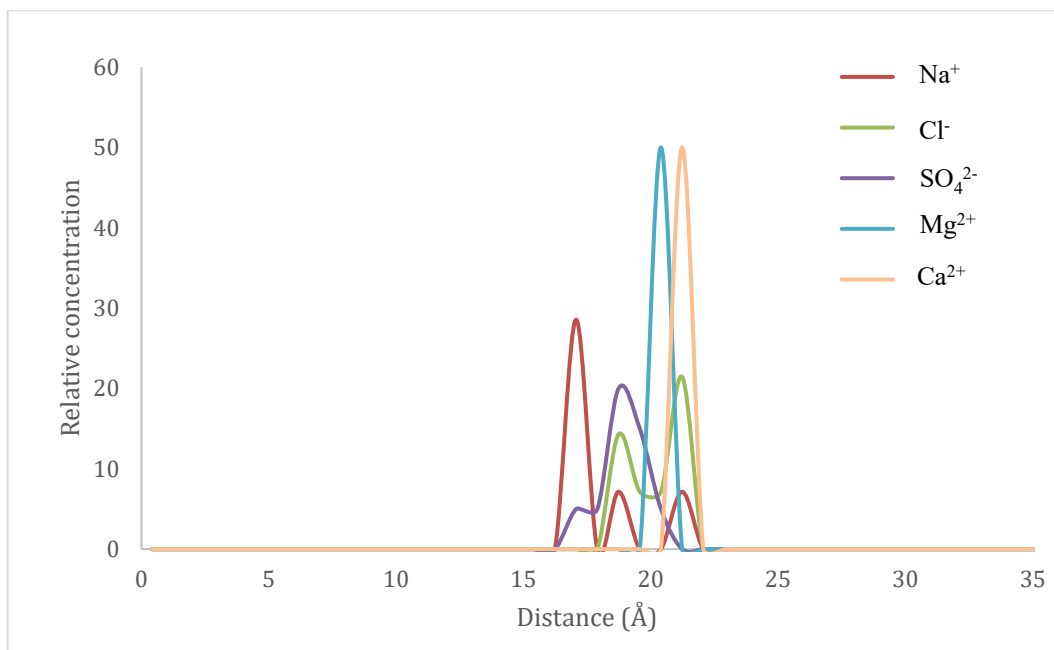


Figure 19. Concentration profile of ions in HS brine

For LS brine, the Stern layer, which consists of Na^+ ions, is located further from the surface compared to the Stern layer in HS brine. The main difference between the distribution of ions given in Figures 19 and 20 is as follows: for LS brine Na^+ ions are distributed 4.9 \AA (Figure 20) away from the rock surface compared to 2 \AA for HS brine (Figure 19). The fact that Na^+ ions are more distributed in the bulk rather than interface in LS brine compared to the high distribution of the Na^+ ions at the interface in HS brine can be explained by denser first water monolayer for HS brine which contributes to energy penalty required for a restructuring of the solvation shell of the Na^+ ions (Koleini et al, 2018).

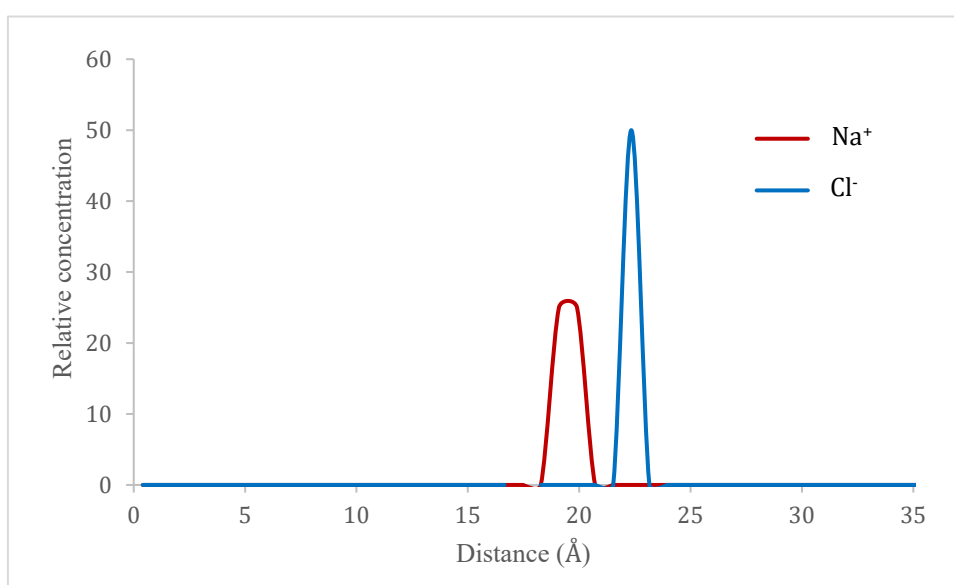


Figure 20. Concentration profile of ions in HS brine

EDL could be observed for both LS and HS brines. The Na^+ ions make up the Stern layer in both cases. This can be explained by the fact that $\{1014\}$ cleavage plane of the calcite crystal carries partial negative charge because outermost atoms of the surface are the sets of oxygen atoms of the carbonate group. This negative charge attracts polar water molecules to the surface of the rock, thus forming a highly ordered first adsorption layer. Water molecules in this layer arrange themselves in a highly ordered manner by facing their oxygen atom towards the bulk of the liquid. The polarity created by these water molecules is ideal for adsorption of positively charged Na^+ ions. After that comes the diffuse layer which mainly consists of Cl^- ions. However, when brine contains sulfate ions, like in the case with HS brine, sulfate ions appear in the diffuse layer and increase its overall charge. The stronger attraction caused by the presence of sulfate ions is the reason for the shrinkage brine layer. The short water layer contributes to the attraction of negatively charged carboxylic groups on heptanoic acid and positively charged stern layer making the surface more oil-wet. Water thickness can be increased by decreasing charges carried by Stern and diffuse layers through ion tuning.

5.5 Distribution of polar components in oil

The relative concentration of polar components in oil (heptanoic acid) is given in Figures 21. As can be seen from these figures heptanoic acid molecules tend to arrange themselves towards the interface between the oil and water phases. These can be explained by attractive forces between charged sites on the surface and polar oil components, like heptanoic acid. The concentration of heptanoic acid at the interface was much larger with HS brine compared to less saline brines. This is attributed to the presence of divalent cations in the bulk of the brine, which attracts negatively charged carboxylic group on the acid molecule. This result correlates with the MIE mechanism proposed by Lager et al (2008). According to the authors, organometallic bridges are responsible for adhesion of polar components in the oil to the oil-brine interface, which makes the surface more oil-wet. However, the authors supposed that the adhesion of the oil components occurs only when water film on the rock ruptures. This work shows that the rupture of water film is not required for attachment of oil components on the surface.

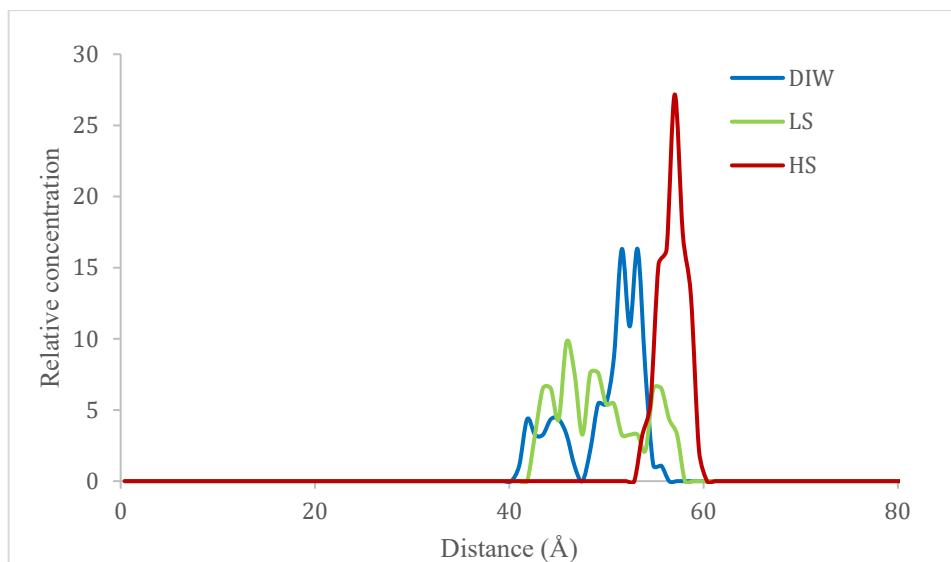


Figure 21. Concentration profile of heptanoic acid molecules for HS case

5.6 Interaction energy

The calculations for interaction energy are given in Appendix A. The results for the calculation of interaction energy are given in Table 2. ΔE is the difference between oil-calcite interaction energy and water-calcite interaction energy. Positive ΔE indicates that interaction energy between water and calcite is larger than interaction energy between oil and calcite. As can be seen from the table, ΔE is the smallest for the case with HS brine, which indicates that the surface is more oil-wet compared to other cases. However, ΔE is found to be larger for brine with low salinity than for deionized brine, which means that surface covered with LS brine is more water-wet compared to the surface covered with DIW.

Table 2. Results for calculation of the difference in interaction energy.

Brine salinity	DIW	LS	HS
ΔE (kcal/mol)	3008	4209	2170

5. Conclusions and Recommendations

The main objectives of this research work were investigation of the effect of brine composition on brine film stability and analyzing the behavior of the individual ions during LSW. The following 4 conclusions can be drawn from the results obtained from this molecular dynamics simulation study:

1. As the salinity of brine decreases, water film on the calcite surface expands. Water film expanded by 21% when the salinity of brine was decreased from 130,000 ppm to 21,000 ppm and by another 10% when the salinity of brine was decreased to 0 ppm.
2. The formation of EDL was verified for the system with HS brine. The second adsorption layer consisted of Na^+ ions which formed a positive Stern layer. This was followed by a diffuse layer which consisted of Cl^- and SO_4^{2-} ions. The Ca^{2+} and Mg^{2+} ions did not appear in the electric double layer and were furthest from the surface. This can be explained by their larger hydration shell.
3. For LS brine, the Stern layer which consisted of Na^+ ions was located further from the rock surface compared to the Stern layer in HS brine. This was attributed due to the larger first adsorption layer which consisted of water molecules.
4. The acid molecules in the oil coordinated themselves towards the oil-brine interface. In HS brine, the concentration of acid molecules at the interface was larger compared to other brines, which can be explained by the presence of divalent cations in the outer shell of the brine. This agrees with the mechanism proposed by Lager et al (2008), where the attachment of polar components in the oil to the oil-water interface was explained by organometallic bridges.

To further improve this work, it is recommended to increase the size of the simulation box, which could not be done with the current computational power that we possess. This will allow getting more accurate results. The more accurate result can be achieved by simulating a larger number of ions and for longer simulation steps. Another issue is that MDS cannot simulate the chemical interaction between the rock and brine phases, which makes the modeling of the dissolution mechanism by MDS impossible.

Nomenclature

Acronyms and Abbreviations

COMPASS	Condensed-phase optimal molecular potential for atomistic simulation studies
DIW	Deionized water
DLE	Double layer expansion
EDL	Electrical double layer
EOR	Enhanced oil recovery
FW	Formation water
HS	High salinity
IEP	Iso-electric point
IFT	Interfacial tension
IOR	Improved oil recovery
LS	Low salinity
LSW	Low salinity waterflooding
MDS	Molecular dynamic simulation
MIE	Multicomponent ion exchange

Symbols

c	Concentrations of the carboxylic group, (mol/L) or (ppm)
c_{ww}	Concentrations of the carboxylic group in water-wet conditions, (mol/L) or (ppm)
c_{ow}	Concentrations of the carboxylic group in oil-wet conditions, (mol/L) or (ppm)
E_{angle}	Angle potential, (cal/mol) or (J/mol)
E_{bond}	Bond potential, (cal/mol) or (J/mol)
$E_{intramolecular}$	Intramolecular potential, (cal/mol) or (J/mol)
$E_{torsion}$	Torsional potential, (cal/mol) or (J/mol)
E_{O-c}	Interaction energy between molecules in the oleic phase and calcite molecules, (kcal/mol) or (kJ/mol)
E_{O+c}	Total energy of a system containing only oil and calcite molecules, (kcal/mol) or (kJ/mol)
E_{W-c}	Interaction energy between water and calcite molecules, (kcal/mol) or (kJ/mol)
E_{W+c}	Total energy of a system containing only water and calcite molecules, (kcal/mol) or (kJ/mol)

E_C	Total energy of calcite molecules, (kcal/mol) or (kJ/mol)
E_O	Total energy of oil molecules, (kcal/mol) or (kJ/mol)
E_W	Total energy of water molecules, (kcal/mol) or (kJ/mol)
$E_{Coulomb}$	Coulomb potential, (cal/mol) or (J/mol) or (kJ/mol)
E_{LJ}	Lennard-Jones potential, (cal/mol) or (J/mol) or (kJ/mol)
F	Weighing factor
$k_{ro,ow}^*$	Relative permeability of oil in oil-wet condition
$k_{ro,ww}^*$	Relative permeability of oil in water-wet condition
$k_{rw,ow}^*$	Relative permeability of water in oil-wet condition
$k_{rw,ww}^*$	Relative permeability of water in water-wet condition
k^{HS}	Relative permeability in high salinity water
k^{LS}	Relative permeability in low salinity water
k_r	Stiffness parameter of the bond, (cal/mol.m ²) or (J/mol.m ²)
k_θ	Stiffness parameter of the angle, (cal/mol.degree ²) or (J/mol. degree ²)
$k_{\phi,m}$	Stiffness parameter of torsion of the bond, (cal/mol.degree ²) or (J/mol. degree ²)
r	Distance between particles, (nm)
r_{ij}	Bond length, (nm)
r_0	Bond equilibrium length, (nm)
$q_{1,2}$	Charge of the particle, (C)
S	Saturation of the phase

Greek Letters

β_{Ca}	Amount of adsorbed Ca ²⁺ ions, (mg)
β_{Mg}	Amount of adsorbed Mg ²⁺ ions, (mg)
γ_m	Equilibrium angle between two planes, (degrees)
ΔE	Difference between interaction energies, (kcal/mol)
ε	Depth of potential well, (kcal/mol)
ε_0	Permittivity of the medium, (F/m)
θ	Wettability indicator
θ_0	Equilibrium angle between two bonds, (degree)
θ_{ijl}	Angle between two bonds, (degree)
σ	Distance between two particles, (nm)
ϕ_{ijk}	Angle between two intersecting planes, (degree)

Metric Conversion Factors

$$1 \text{ \AA} = 10^{-10} \text{ m}$$

$$1 \text{ cal} = 4.184 \text{ J}$$

$$^{\circ}\text{F} = (^{\circ}\text{C} \times 1.8) + 32$$

$$1 \text{ cal} = 4.184 \text{ J}$$

$$1 \text{ ppm} = 1 \text{ mg/L}$$

6. References

- Al-Attar, H H, Mahmoud, M Y, Zekri, A. Y, Almehaideb, R A and Ghannam, M T, 2013. Low salinity flooding in a selected carbonate reservoir: experimental approach, paper presented to the EAGE Annual Conference & Exhibition, London, United Kingdom, 10-13 June.
- Awolayo, A, Sarma, H K, and AlSumaiti, A. M, 2014. A laboratory study of ionic effect of smart water for enhancing oil recovery in carbonate reservoirs, paper presented to the SPE EOR Conference at Oil and Gas West Asia, Muscat, Oman, 31 March – 2 April.
- Barrat, J and Hansen, J, 2003. *Basic concepts for simple and complex liquids*, 4 p (Cambridge University Press: Cambridge).
- Bartels, W, Mahani, H, Berg, S and Hassanizadeh, G S, 2019. Literature review of low salinity waterflooding from a length and time scale perspective, *Fuel*, 236:338-353.
- Bavière, M, 1991. *Basic concepts in enhanced oil recovery processes*, 48 p (Blackwell: Oxford).
- Chandrasekhar, S and Mohanty, K K, 2013. Wettability alteration with brine composition in high temperature carbonate reservoirs, paper presented to SPE Annual Technical Conference and Exhibition, New Orleans, USA, 30 September – 2 October.
- Chen, H, Panagiotopoulos, A Z and Giannelis, E P, 2015. Atomistic molecular dynamics simulations of carbohydrate-calcite interactions in concentrated brine, *Langmuir*, 3:2407–2413.
- Emad, A, and Sepehrnoori, K, 2016. A comprehensive review of low salinity/engineered water injections and their applications in sandstone and carbonate rocks, *Journal of Petroleum Science and Engineering*, 139:137-161.
- Emadi, A and Sohrabi, M, 2013. Visual investigation of oil recovery by low salinity water injection: formation of water microdispersions and wettability alteration, paper presented to the SPE Annual Technical Conference and Exhibition, New Orleans, USA, 30 September–2 October.
- Fathi, S J, Austad, T and Strand, S, 2011. Water-based enhanced oil recovery by “smart water”: optimal ionic composition for EOR in carbonates, *Energy & Fuels*, 25(11):5173-5179.
- Fenter, P S, Kerisit, P, Raiteri, J and Gale, D, 2013. Is the calcite-water interface understood? Direct comparisons of molecular dynamics simulations with specular X-ray reflectivity data, *J. Phys. Chem. C*, 117:5028–5042.

- Fjelde, I, Asen, S V and Omekeh, A, 2012. Low salinity water flooding experiments and interpretation by simulations, paper presented to the Eighteenth SPE Improved Oil Recovery Symposium, Tulsa, USA, 14-18 April.
- Greathouse, J A, Cygan, R T, Fredrich, J T and Jerauld, G R, 2017. Adsorption of aqueous crude oil components on the basal surfaces of clay minerals: molecular simulations including salinity and temperature effects, *Journal of Physical Chemistry*, 121:22773-22786.
- Gupta, R, Smith, G G, Hu, L, Willingham, G T, Cascio, M L, Shyeh, J J and Harris, C R, 2011. Enhanced waterflood for middle east carbonates cores – impact of injection water composition, paper presented to the Middle East Oil and Gas Show and Conference, Manama, Bahrain, 25-28 September.
- Hognesen, E J, Strand, S and Austad, T, 2005. Waterflooding of preferential oil-wet carbonates: oil recovery related to reservoir temperature and brine composition, paper presented to the SPE EUROPEC/EAGE Annual Conference, Madrid, Spain, 13-16 June.
- Karimi, M, Al-Maamari, R S, Ayatollahi, S and Mehranbod, N, 2016. Impact of sulfate ions on wettability alteration of oil-wet calcite in the absence and presence of cationic surfactant, *Energy Fuels*, 30:819–829.
- Kerisit, V and Parker, S C, 2004. Free energy of adsorption of water and metal ions on the {1014} calcite surface, *J. Am. Chem. Soc.*, 126:10152–10161.
- Khanamiri, H H, Khaledialidusti, R, Torsaeter, O and Stensne, J A, 2014. Nano-scale modeling of rock-fluid interactions in low salinity water imbibition, paper presented to International Symposium of the Society of Core Analysis, Avignon, France, 8-11 September.
- Lager, A, Webb, K J and Black, C J J, 2007. Impact of brine chemistry on oil recovery, paper presented to the 14th European Symposium on IOR, Cairo, Egypt, 22-24 April.
- Lager, A, Webb, K J, Black, C J J, Singleton, M and Sorbie, K S, 2008. Low salinity oil recovery - an experimental investigation, *Petrophysics*, 41(1):28-35.
- Leach, A, 2001. *Molecular modelling*, pp 318-361 (Pearson/Prentice Hall: Harlow).
- Lee, S Y, Webb, K J, Collins, I, Lager, A and Clarke, S, 2010. Low salinity oil recovery: increasing understanding of the underlying mechanisms, paper presented to the SPE Improved Oil Recovery Symposium, Tulsa, USA, 24-28 April

- Mahani, H, Keya, A L, Berg, S, Bartels, W, Nasralla, R and William, R, 2015. Driving mechanism of low salinity flooding in carbonate rocks, paper presented to the SPE EUROPEC, Madrid, Spain, 1-4 June.
- Mehana, M and Fahes, M M, 2018. Investigation of double layer expansion in low salinity waterflooding: Molecular simulation study, paper presented to the SPE Western Regional Meeting, California, USA, 22-27 April.
- Mwangi, P, Brady, P, Randonjic, M and Thyne, G, 2018. The effect of organic acids on wettability of sandstone and carbonate rocks, *Journal of Petroleum Science and Engineering*, 165:428-435.
- Nasralla, R A and Nasr-El-Din, H A, 2011. Impact of electrical surface charges and cation exchange on oil recovery by low salinity water, paper presented to the SPE Asia Pacific Oil and Gas Conference and Exhibition, Jakarta, 20–22 September.
- Nasralla, R A, Bataweel, M A and Nasr-El-Din, H A, 2011. Investigation of wettability alteration by low salinity water, presented to the Offshore Europe, Aberdeen, UK, 6–8 September.
- Qiao, C, Johns, R and Li, L, 2016. Modeling low-salinity waterflooding in chalk and limestone reservoirs, *Energy & Fuels*, 30(2):884-895.
- Rashid, S, Mousapour, M, Ayatollahi, S, Vossoughi, M and Beigy, A, 2015. Wettability alteration in carbonates during “Smart Waterflood”: Underlying mechanisms and the effect of individual ions. *Colloids and Surfaces A: Physicochemical and Engineering Aspects*, 487:142-153.
- Raymond, M and Leffler, W L, 2006. *Oil and gas production in nontechnical language*, p 235-240 (PennWell: Tulsa).
- Ricci M, Spijker, P, Stellacci, F, Molinari, J F and Voïtchovsky, K, 2013. Direct visualization of single ions in the Stern layer of calcite, *Langmuir*, 29:2207–2216.
- Rivet, S M, 2009. Coreflooding oil displacements with low salinity brine, Master Thesis, University of Texas at Austin.
- Saikia, B, Mahadevan, J and Rao, D, 2018. Exploring mechanisms for wettability alteration in low-salinity waterfloods in carbonate rocks, *Journal of Petroleum Science and Engineering*, 164:595-602.

Schembre, J M and Kavscek, A R, 2004. Thermally induced fines mobilization: its relationship to wettability and formation damage, paper presented to the SPE International Thermal Operations and Heavy-Oil Symposium and Western Regional Meeting, California, USA, 16-18 March.

Schembre, J, Tang, G Q and Kavscek, A, 2006. Wettability alteration and oil recovery by water imbibition at elevated temperatures, *Journal of Petroleum Science and Engineering*, 52:131-148.

Secombe, J, Lager, A, Jerauld, G, Jhaveri, B, Buikema, T and Bassler, S, 2010. Demonstration of low-salinity EOR at interwell scale, Endicott Field, Alaska, presented to the SPE Improved Oil Recovery Symposium, Tulsa, USA, 24-28 April.

Skrettingland, K, Holt, T, Tveheyo, M and Skjevraak, I, 2011. Snorre low salinity water injection - core flooding experiments and single well field pilot, *SPE Res Eval & Eng*, 14 (2):182–192.

Sohrabi, M, Mahzari, P, Farzaneh, S A, Mills, J R and Tsoilis, P, 2017. Novel insights into mechanisms of oil recovery by use of low salinity water injection, *Society of Petroleum Engineers*, 22 (2):407-416.

Strand, S, Austad, T, Puntervold, T, Hognesen, E J, Olsen, M and Barstad, S M F, 2008. Smart water for oil recovery from fractured limestone: a preliminary study, *Energy & Fuels*, 22(5):3126-3133.

Strand, S, Puntervold, T and Austad, T, 2008. Effect of temperature on enhanced oil recovery from mixed wet chalk cores by spontaneous imbibition and forced displacement using seawater, *Energy & Fuels*, 22(5):3222-3225.

Suijkerbuijk, B, Sorop, T G, Parker, A R, Masalmeh, S K, Chmuzh, I V, Karpan, V M, 2014. Low salinity waterflooding at west Salym: laboratory experiments and field forecasts, paper presented to the SPE Improved Oil Recovery Symposium, Tulsa, USA, 12-16 April.

Sun, H, 1998. COMPASS: An ab initio force-field optimized for condensed-phase applications - overview with details on alkane and benzene compounds, *J. Phys. Chem.*, 102:7338.

Tabrizy, V A, Hamouda, A A and Denoyel, A, 2011. Influence of magnesium and sulfate ions on wettability alteration of calcite, quartz, and kaolinite: surface energy analysis, *Energy Fuels*, 25:1667–1680.

Tang, G and Kovscek, A R, 2004. An experimental investigation of the effect of temperature on recovery of heavy-oil from diatomite, *SPE Journal*, 9(2):163-179.

Tang, G Q and Morrow, N R, 1999. Influence of brine composition and fine migration on crude oil/brine/rock interactions and oil recovery, *J. Pet. Sci. Eng.*, 24(24):99–111.

Tirjoo, A, Bayati, B, Rezaei, H and Rahmati, M, 2019. Molecular dynamics simulation of the effect of ions in water on the asphaltene aggregation, *Journal of Molecular Liquids*, 277:40-48.

Webb, K J, Black, C J J and Tjetland, G, 2005. A laboratory study investigating methods for improving oil recovery in carbonates, paper presented to the SPE International Petroleum Technology conference, Doha, Qatar, 21-23 November.

Xie, Q, Liu, Y, Wu, J and Liu, Q, 2014. Ions tuning water flooding experiments and interpretation by thermodynamics of wettability, *J. Petroleum Sci. Eng.*, 124:350-358.

Yousef, A A, Al Saleh, S and Al Jawfi, M, 2012. The impact of the injection water chemistry on oil recovery from carbonate reservoirs, paper presented to the Conference at Oil and Gas West Asia, Muscat, Oman, 16-18 April.

Yousef, A A, Al-Saleh, S, Al-Kaabi, A and Al-Jawfi, M, 2011. Laboratory investigation of the impact of injection-water salinity and ionic content on oil recovery from carbonate reservoirs, *SPE Reservoir Evaluation & Engineering*, 14(5):578-593.

Zahid, A, Shapiro, A and Skauge, A, 2012. Experimental studies of low salinity water flooding in carbonate reservoirs: a new promising approach, paper presented to the Conference at Oil and Gas West Asia, Muscat, Oman, 16-18 April

Zhang, P, Tweheyo, M T and Austad, T, 2006. Wettability alteration and improved oil recovery in chalk: the effect of calcium in the presence of sulfate, *Energy & Fuels*, 20(5):2056-2062.

Zhang, Y, Xie, X and Morrow, N R, 2007. Waterflood performance by injection of brine with different salinity for reservoir cores, paper presented to the SPE Annual Technical Conference and Exhibition, Anaheim, California, USA, 11-14 November.

Zhu, B, Xu, X and Tang, R, 2013. Hydration layer structures on calcite facets and their roles in selective adsorptions of biomolecules: a molecular dynamics study, *J. Chem. Phys.*, 139(23):234705.

APPENDIX A

Table 3. Calculation for the difference in interaction energy

Salinity	E_s (kcal/mol)	E_w (kcal/mol)	E_D (kcal/mol)	E_{D+s} (kcal/mol)	E_{w+s} (kcal/mol)	ΔE (kcal/mol)
DIW	-216050	-3592	-714	-216743	-222629	3008
LS	-349803	-2798	-787	-350609	-348373	4209
HS	-216049	36	-364	-216711	-218450	2170